Supporting Information

Porphyrin–Hexaphyrin Hybrid Tapes

Takayuki Tanaka,[†] Naoki Aratani,[†#] Jong Min Lim,[‡] Kil Suk Kim,[‡] Dongho Kim[‡]* and Atsuhiro Osuka[†]*

[†]*Department of Chemistry, Graduate School of Science, Kyoto University, Sakyo-ku, Kyoto 606-8502 (Japan)*

[#]*PRESTO, Japan Science and Technology* [‡]*Spectroscopy Laboratory for Functional π-Electronic Systems and Department of Chemistry, Yonsei University, Seoul 120-749, Korea*

E-mail: aratani@kuchem.kyoto-u.ac.jp; osuka@kuchem.kyoto-u.ac.jp; dongho@yonsei.ac.kr

Contents

1. Instrumentation and Materials

All solvents for reaction were distilled over CaH_2. All reagents were of the commercial reagent grade and were used without further purification except where noted. The spectroscopic grade dichloromethane was used as solvent for all spectroscopic studies. Silica gel column chromatography was performed on Wakogel C-300. Thin-layer chromatography (TLC) was carried out on aluminum sheets coated with silica gel 60 F254 (Merck 5554). UV-visible spectra were recorded on a Shimadzu UV-3100PC spectrometer. ^1H and ^{19}F NMR spectra were recorded on a JEOL ECA-600 spectrometer (operating as 600.17 MHz for ^1H and 565 MHz for ^{19}F) using the residual solvent as the internal reference for ^1H (d = 7.26 ppm in $CDCl_3$, d = 7.16 ppm in C_6D_6, and d = 1.72 ppm in [D_8]THF), and hexafluorobenzene as the external reference for ^{19}F (d= –162.9 ppm). High-resolution electrospray-ionization time-of-flight mass spectroscopy (HR-ESI-TOF-MS) was recorded on a BRUKER microTOF model using positive and negative mode for acetonitrile solutions of samples. Redox potentials were measured by cyclic voltammetry on an ALS electrochemical analyzer model 660. All calculations were carried out using the Gaussian 09 program.[S1]

2. Experimental Section

10,15,20-Tris(3,5-di-*tert*-butylphenyl)-5-formyl Ni^{II} porphyrin (1).

N,N-Dimethylformamide (5.4 mL, 20 eq) in the round-bottomed-flask was added phosphoryl chloride (6.5 mL, 20 eq) at 0 °C. The solution was stirred for 10 min at room temperature. To a solution of 5,10,15-tris(3,5-di-*tert*-butylphenyl) Ni^{II} porphyrin (3.25 g, 0.751 mmol) in CH_2Cl_2 (100 mL) was added the above prepared Vilsmeier reagent slowly at room temperature under nitrogen atmosphere. The solution was refluxed overnight and the dark green solution was diluted with a saturated aqueous solution of $NaHCO_3$ (200 mL) and maintained at room temperature whilst stirring for further 2 h. The organic phase was separated, washed with H_2O, dried over anhydrous Na_2SO_4 and evaporated in vacuo. Purification of the residue by silica-gel column chromatography with a mixture of CH_2Cl_2 and *n*-hexane (*v/v* = 1/1) as an eluent afforded 3.3 g (98%) of **1**.

^{1}H NMR ($CDCl_3$): δ 12.05 (s, 1H, CHO), 9.79 (d, *J* = 5.0 Hz, 2H, β), 8.88 (d, *J* = 5.0 Hz, 2H, β), 8.68 (d, *J* = 5.0 Hz, 2H, β), 8.62 (d, *J* = 5.0 Hz, 2H, Ar), 7.80 (m, 6H, Ar), 7.73 (m, 2H, Ar), 7.70 (m, 1H, Ar), 1.47 (s, 36H, *t*-Bu), and 1.45 (s, 18H, *t*-Bu) ppm; MS (MALDI-TOF): calcd for $C_{63}H_{72}N_4NiO$ 960.0; found: 960.5 ;UV-Vis ($CHCl_3$) λ_{max} = 429, 556, and 599 nm.

Ni^{II} [10,15,20-tris(3,5-di-*tert*-butylphenyl)]porphyrinyl dipyrromethane (2).

To a solution of **1** (1.92 g, 2.00 mmol) and pyrrole (55.5 mL, 0.800 mol) was added trifluoroacetic acid (0.15 mL, 2.00 mmol) and stirrd for 1 h at room temperature under nitrogen. After neutralization with 1N NaOHaq. (2.0 mL), the solution was extracted with CH_2Cl_2, dried over anhydrous Na_2SO_4 and evaporated in vacuo. Unreacted pyrrole was distilled under vacuum and the residue was purified by silica-gel column chromatography with a mixture of CH_2Cl_2 and *n*-hexane (*v/v* = 1/1) as an eluent. Recrystallization from CH_2Cl_2/MeOH gave red solid **2** (1.55 g, 72% yield).

^{1}H NMR (C_6D_6): δ 9.26 (d, *J* = 5.0 Hz, 2H, β), 9.06 (d, *J* = 4.8 Hz, 2H, β), 9.04 (d, *J* = 4.8 Hz, 2H, β), 8.97 (d, *J* = 5.0, 2H, β), 8.12 (s, 2H, Ar), 8.10 (s, 2H, Ar), 7.54 (s, 1H, CH), 7.43 (s, 1H, NH), 6.48 (m, 2H, pyrrole-H), 6.38 (dd, 2H, pyrrole-H), 6.31 (m, 2H, pyrrole-H), 1.50 (s, 18H, *t*-Bu), and 0.50 (s, 36H, *t*-Bu) ppm; ^{13}C NMR ($CDCl_3$): δ 149.37, 142.78, 142.66, 142.57, 141.77, 139.78, 135.45, 134.02, 133.08, 132.76, 130.66, 128.86, 128.80, 121.56, 121.51, 120.12, 117.31, 108.92, 107.69, 43.61, 35.32, and 32.01 ppm; HR-ESI-MS m/z = 1111.5517, calcd for $C_{71}H_{80}N_6NiCl$ = 1111.5474 $[M+Cl]^-$; UV-Vis ($CHCl_3$) $\lambda_{max}(\varepsilon\,[M^{-1}cm^{-1}])$ = 424 (251000), and 537 nm (16000).

10,15,20-Tris(3,5-di-*tert*-butylphenyl) Ni^{II} porphyrinyl-pentakis(pentafluorophenyl) [26]hexaphyrin (3).

To a solution of pentafluorobenzaldehyde (0.138 mL, 1.1 mmol, 3 eq) in CH_2Cl_2 (16 mL) was added $BF_3\cdot OEt_2$ (0.028 mL, 0.22 mmol, 0.6 eq) and the resulting solution was stirred for 15 min at 0 °C. A solution of pentafluorophenyl dipyrromethane (232 mg, 0.74 mmol, 2 eq) and **2** (400 mg, 0.37 mmol, 1 eq) in CH_2Cl_2 (17.2 mL) was transferred to the pre-activated aldehyde solution at room temperature and the mixture was stirred for 30 min under nitrogen. After addition of 2,3-dichloro-5,6-dicyano-1,4-benzoquinone (DDQ) (845 mg, 3.7 mmol, 10 eq), the solution was stirred for 1 h and passed through an alumina column for neutralization and removal of tar. After the solution was evaporated to dryness, the residue was separated by silica-gel column chromatography, at first with a mixture of CH_2Cl_2 and *n*-hexane (30:70) as an eluent. The first red fraction was *meso-meso* linked porphyrin trimer **5** and the second red fraction was *meso-meso* linked porphyrin dimer **4**. Next, column chromatography with a mixture of CH_2Cl_2 and *n*-hexane (50:50) gave a purple fraction of *meso-meso* linked porphyrin-hexaphyrin hybrid **3** along with 5,15-bis(Ni^{II} porphyrin)yl-10,20,25,30-tetrakispentafluorophenyl [26]hexaphyrin, [26]hexaphyrin (29.9 mg, 0.0021 mmol, 5.5%) and many by-products. Yields: **3** (39.4 mg, 0.018 mmol, 4.8%), **4** (86.0 mg, 0.049 mmol, 13.3%), and **5** (24.5 mg, 0.0098 mmol, 5.3%)

3: ^{1}H NMR ($CDCl_3$, –20 °C): δ 9.56 (d, J = 4.5 Hz, 2H, hexa-β), 9.20 (d, J = 4.5 Hz, 2H, hexa-β), 9.19 (d, J = 4.5 Hz, 2H, hexa-β), 9.00 (d, J = 4.9 Hz, 2H, por-β), 8.94 (d, J = 4.9 Hz, 2H, β), 8.78 (d, J = 5.0 Hz, 2H, por-β), 8.57 (d, J = 4.5 Hz, 2H, hexa-β), 8.18 (d, J = 5.0 Hz, 2H, por-β), 8.00 (s, 2H, Ar), 7.93 (s, 4H, Ar), 7.78 (s, 1H, Ar), 7.65 (s, 2H, Ar), 1.54 (s, 18H, *t*-Bu), 1.42 (s, 36H, *t*-Bu), –1.85 (s, 1H, NH), –2.35 (s, 1H, NH), –2.40 (d, J = 3.4 Hz, 2H, inner-β), and –2.54 (d, J = 3.4 Hz, 2H, inner-β) ppm; ^{19}F NMR ($CDCl_3$): δ –136.2 (dd, 2F, Ar-*o*), –136.8 (d, 8F, Ar-*o*), –150.06 (t, 1F, Ar-*p*), –153.1 (q, 8F, Ar-*p*), –160.4 (td, 2F, Ar-*m*), and –163.1 (tt, 8F, Ar-*m*); HR-ESI-MS m/z = 2225.6022, calcd for $C_{122}H_{85}F_{25}N_{10}Ni$ = 2225.6018 $[M]^+$;UV-Vis ($CHCl_3$) $\lambda_{\mathrm{max}}(\varepsilon\ [\mathrm{M^{-1}cm^{-1}}])$ = 419 (178000), 572 (172000), 729 (33000), 892 (15000) and 1029 (9000) nm.

4; ^{1}H NMR ($CDCl_3$): δ 8.94 (d, J = 6.4 Hz, 4H, β), 8.91 (d, J = 5.0 Hz, 2H, β), 8.87 (d, J = 4.8 Hz, 2H, β), 8.61 (d, J = 5.1 Hz, 2H, β), 8.54 (d, J = 4.7 Hz, 2H, β), 8.25 (d, J = 4.8 Hz, 2H, β), 7.97 (s, 2H, Ar), 7.97 (d, J = 5.0 Hz, 2H, β), 7.88 (d, J = 1.6 Hz, 4H, Ar), 7.77 (t, 1H, Ar), 7.65 (s, 2H, Ar), 1.40 (s, 36H, *t*-Bu), 1.26 (s, 18H, *t*-Bu), and –2.41 (s, 2H, NH) ppm; ^{19}F NMR ($CDCl_3$): δ –136.4 (m, 6F, Ar-*o*), –151.5 (t, 1F, Ar-*p*), –151.7 (t, 2F, Ar-*p*), –161.4 (td, 2F, Ar-*m*), and –161.6 (td, 4F, Ar-*m*); HR-ESI-MS m/z = 1735.5590, calcd for $C_{100}H_{80}F_{15}N_8Ni$ = 1736.5647 $[M]^-$; UV-Vis ($CHCl_3$) λ_{max} $(\varepsilon\ [\mathrm{M^{-1}cm^{-1}}])$ = 417 (263000), 429 (281000), 510 (36000), 537 (33000), 590 (16000), and 645 nm (4000).

5; ^{1}H NMR ($CDCl_3$): δ 8.92 (d, J = 6.4 Hz, 4H, β), 8.88 (d, J = 5.0 Hz, 4H, β), 8.65 (d, J = 4.8 Hz, 4H, β), 8.56 (d, J = 4.6 Hz, 4H, β), 8.28 (d, J = 5.0 Hz, 4H, β), 8.10 (d, J = 4.8 Hz, 4H, β), 7.99 (d, J = 1.9 Hz, 4H, Ar), 7.91 (d, J = 1.9 Hz, 8H, Ar), 7.77 (t, 2H, Ar), 7.67 (t, 4H, Ar), 1.42 (s, 72H, *t*-Bu), 1.26 (s, 36H, *t*-Bu), and –1.91 (s, 2H, NH) ppm; ^{19}F NMR ($CDCl_3$): δ –136.2 (dd, 2F, Ar-*o*), –136.8 (d, 8F, Ar-*o*), –150.06 (t, 1F, Ar-*p*), –153.1 (q, 8F, Ar-*p*), –160.4 (td, 2F, Ar-*m*), and –163.1 (tt, 8F, Ar-*m*); HR-ESI-MS m/z = 2525.0731, calcd for $C_{156}H_{152}F_{10}N_{12}Ni_2Na$ = 2525.0731 $[M+\mathrm{Na}]^+$; UV-Vis ($CHCl_3$) λ_{max} $(\varepsilon\ [\mathrm{M^{-1}cm^{-1}}])$ = 417 (298000), 540 (70000), 596 (27000), and 652 nm (9000).

***meso-meso*, *β-β*, *β-β* Triply linked porphyrin–[26]hexaphyrin hybrid 6**.

To a solution of **3** (8.5 mg, 3.8 μmol) in dry toluene (10 mL) were added DDQ (4.3 mg, 5 eq) and $Sc(OTf)_3$ (9.4 mg, 5 eq), and the resulting mixture was stirred at 80 °C for 5 h. The solution was passed through an alumina column with THF as an eluent. The fraction was evaporated, and purified by an alumina column or silica-gel short column using CH_2Cl_2 as an eluent. A dark purple solution of **6** (6.1 mg, 72%) was obtained, which can be recrystallized from $CHCl_3$/EtOH.

^{1}H NMR ($CDCl_3$): δ 8.56 (d, J = 4.7 Hz, 2H, hexa-β), 8.27 (d, J = 4.7 Hz, 2H, hexa-β), 7.69 (s, 2H, bay-area-β), 7.63 (t, J = 1.8 Hz, 2H, Ar), 7.54 (t, J = 1.8 Hz, 1H, Ar), 7.45 (d, J = 1.9 Hz, 2H, Ar), 7.37 (d, J = 1.9 Hz, 2H, Ar), 7.17 (d, J = 4.8 Hz, 2H, por-β), 7.09 (d, J = 4.8 Hz, 4H, por-β), 7.08 (s, 2H, bay-area-β) 1.46 (s, 36H, *t*-Bu), 1.37 (s, 18H, *t*-Bu), 0.52 (d, J = 4.4 Hz, 2H, inner-β), and 0.41 (d, J = 4.4 Hz, 2H, inner-β) ppm; ^{19}F NMR ($CDCl_3$): δ –136.5 (dd, 2F, Ar-*o*), –137.0 (dd, 8F, Ar-*o*), –150.7 (t, 1F, Ar-*p*), –153.8 (m, 8F, Ar-*p*), –160.5 (t, 2F, Ar-*m*), and –163.3 (td, 8F, Ar-*m*); HR-ESI-MS m/z = 2219.5712, calcd for $C_{122}H_{81}F_{25}N_{10}Ni$ = 2219.5627 $[M]^-$;UV-Vis ($CHCl_3$) $\lambda_{\mathrm{max}}(\varepsilon\ [\mathrm{M^{-1}cm^{-1}}])$ = 414 (52000), 532 (70000), 566 (74000), 752 (83000), and 1333 nm (19000).

***meso-meso*, *β-β*, *β-β* Triply linked porphyrin–[28]hexaphyrin hybrid (7)**.

To a solution of **6** in CH_2Cl_2/MeOH (*v/v* = 10/1) was added $NaBH_4$ at 0 °C and the mixture was stirred for 1 h. The reaction mixture was quenched by addition of water, extracted with CH_2Cl_2, dried over anhydrous Na_2SO_4 and evaporated to dryness. A dark purple solution of **7** was obtained almost quantitatively.

^{1}H NMR ($CDCl_3$, rt): δ 10.77 (br, 2H, outer NH), 7.93 (d, J = 4.9 Hz, 2H, por-β), 7.87 (d, J = 4.9 Hz, 4H, por-β + por-bay-area-β), 7.64 (m, 2H, Ar), 7.61 (d, J = 1.9 Hz, 4H, Ar), 7.59 (s, 3H, Ar), 7.13 (br, 2H, inner-β), 6.77 (br, 2H, inner-β), 6.70 (s, 2H, hexa-bay-area-β), 6.63 (d, J = 5.0 Hz, 2H, hexa-β), 6.56 (d, J = 5.0 Hz, 2H, hexa-β), 1.43 (s, 36H, *t*-Bu), and 1.39 (s, 18H, *t*-Bu); ^{19}F NMR ($CDCl_3$): δ –136.3 (d, 4F, Ar-*o*), –137.2 (d, 4F, Ar-*o*), –137.6 (d, 2F, Ar-*o*), –150.7 (td, 4F, Ar-*p*), –153.1 (t, 1F, Ar-*p*), –159.7 (t, 4F, Ar-*m*), –160.0 (t, 4F, Ar-*m*), and –161.0 (td, 2F, Ar-*m*); HR-ESI-MS m/z = 2221.5748, calcd for $C_{122}H_{83}F_{25}N_{10}Ni$ = 2221.5783 $[M]^+$;UV-Vis ($CHCl_3$) $\lambda_{max}(\varepsilon\,[M^{-1}cm^{-1}])$ = 399 (48000), 546 (68000), 669 (79000), 793 (77000) and 1310 nm (11000).

Spectral Data for 7 in C_6D_6 and [D$_8$]THF; ^{1}H NMR (C_6D_6, rt): δ 10.24 (br, 2H, NH), 8.20 (s, 2H, por-bay-area β), 8.09 (d, J = 5.0 Hz, 2H, por-β), 8.04 (d, J = 5.0 Hz, 2H, por-β), 7.80 (d, J = 1.6 Hz, 2H, Ar), 7.77 (d, J = 1.6 Hz, 4H, Ar), 7.76 (m, 1H, Ar), 7.71 (m, 2H, Ar), 6.69 (d, J = 4.5 Hz, 2H, hexa-β), 6.61 (br, 2H, hexa-inner-β), 6.57 (s, 2H, hexa-bay-area-β), 6.54 (d, J = 4.5 Hz, 2H, hexa-β), 6.18 (br, 2H, hexa- inner-β), 1.34 (s, 18H, *t*-Bu), and 1.27 (s, 36H, *t*-Bu); ^{1}H NMR ([D$_8$]THF, rt): δ 13.03 (s, 2H, inner NH), 12.81 (s, 2H, inner NH), 10.94 (s, 2H, NH), 8.67(s, 2H, por-bay-area-β), 8.45 (d, J = 5.2 Hz, 2H, por-β), 8.39 (d, J = 5.2 Hz, 2H, por-β), 7.91 (s, 4H, Ar), 7.87 (m, 5H, Ar), 7.46 (br, 2H, NH), 6.57 (s, 2H, hexa-bay-area-β), 5.57 (s, 2H, hexa-β), 5.46 (s, 2H, hexa-β), 1.56 (s, 18H, *t*-Bu), and 1.55 (s, 36H, *t*-Bu)

Femtosecond Transient Absorption Measurements. The femtosecond time-resolved transient absorption (TA) spectrometer pumped by a Ti:sapphire regenerative amplifier system (Quantronix, Integra-C) operating at 1 kHz repetition rate and an optical detection system. The frequency doubled 400 nm pulses had a pulse width of ~ 100 fs and an average power of 1 mW which were used as pump pulses. White light continuum (WLC) probe pulses were generated using a sapphire window (2 mm of thickness) by focusing of small portion of the fundamental 800 nm pulses. The time delay between pump and probe beams was carefully controlled by making the pump beam travel along a variable optical delay (Newport, ILS250). Intensities of the spectrally dispersed WLC probe pulses are monitored by miniature spectrograph (OceanOptics, USB2000+). To obtain the time-resolved transient absorption difference signal (ΔA) at a specific time, the pump pulses were chopped at 25 Hz and absorption spectra intensities were saved alternately with or without pump pulse. Typically, 6000 pulses excite samples to obtain the TA spectra at a particular delay time. The polarization angle between pump and probe beam was set at the magic angle (54.7°) in order to prevent polarization-dependent signals. Cross-correlation fwhm in pump-probe experiments was less than 200 fs and chirp of WLC probe pulses was measured to be 800 fs in the 400-800 nm region. To minimize chirp, all reflection optics in probe beam path and 2 mm path length of quartz cell were used. The three-dimensional data sets of ΔA versus time and wavelength were subjected to singular value decomposition and global fitting to obtain the kinetic time constants and their associated spectra using Surface Xplorer software.

3. NMR Spectra

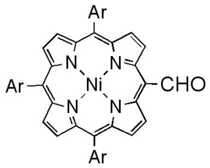

1

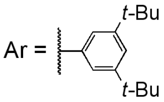

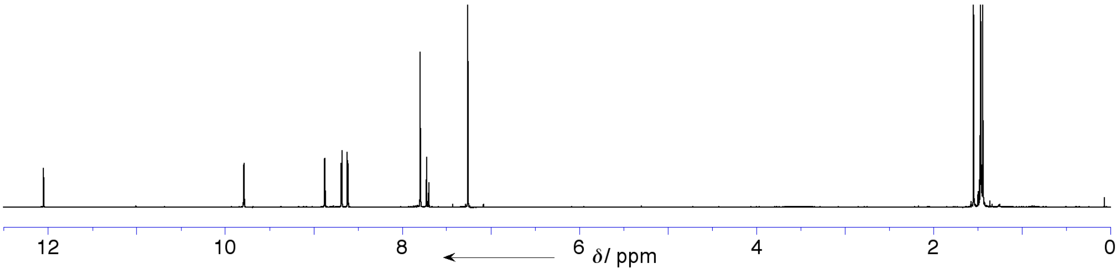

Figure S1. ${}^1H$ NMR spectrum of **1** in $CDCl_3$ at room temperature.

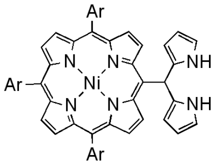

2

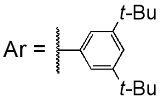

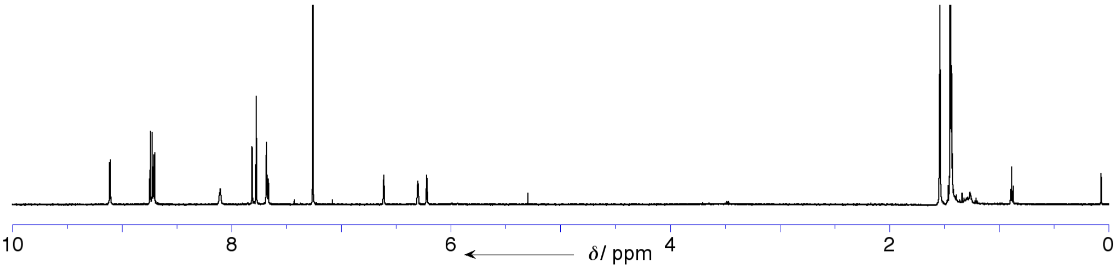

Figure S2. ${}^1H$ NMR spectrum of **2** in $CDCl_3$ at room temperature.

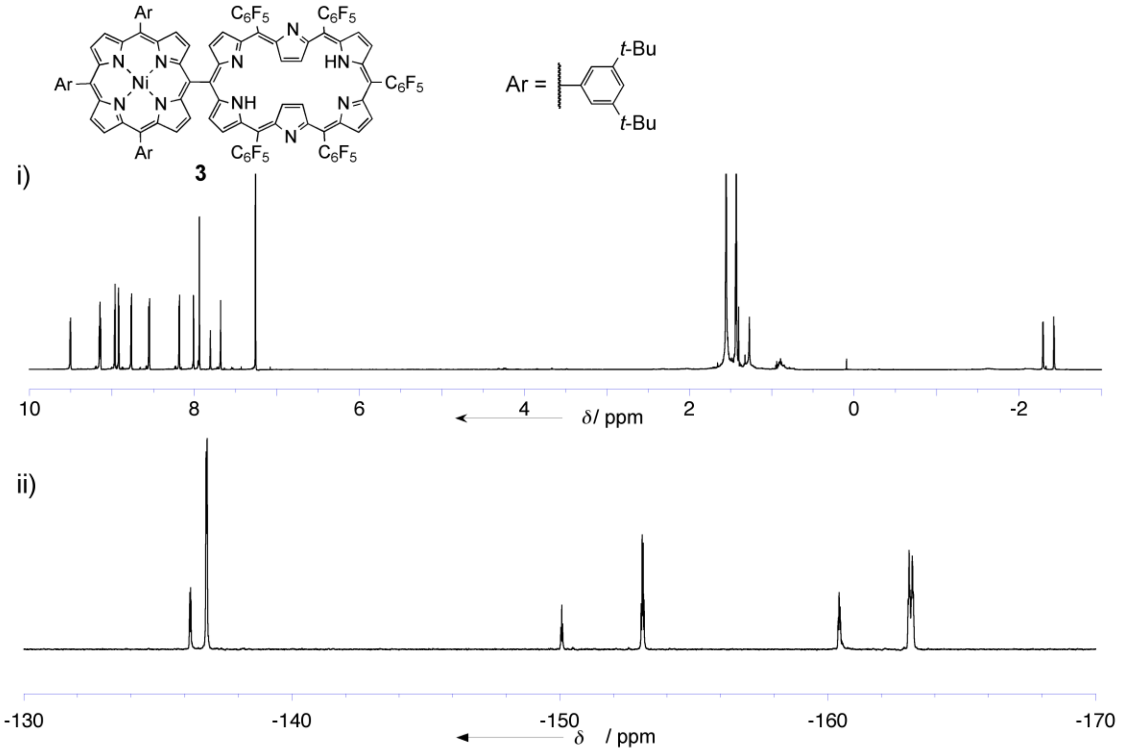

Figure S3. i) ^1H and ii) ^{19}F NMR spectra of **3** in $CDCl_3$ at room temperature.

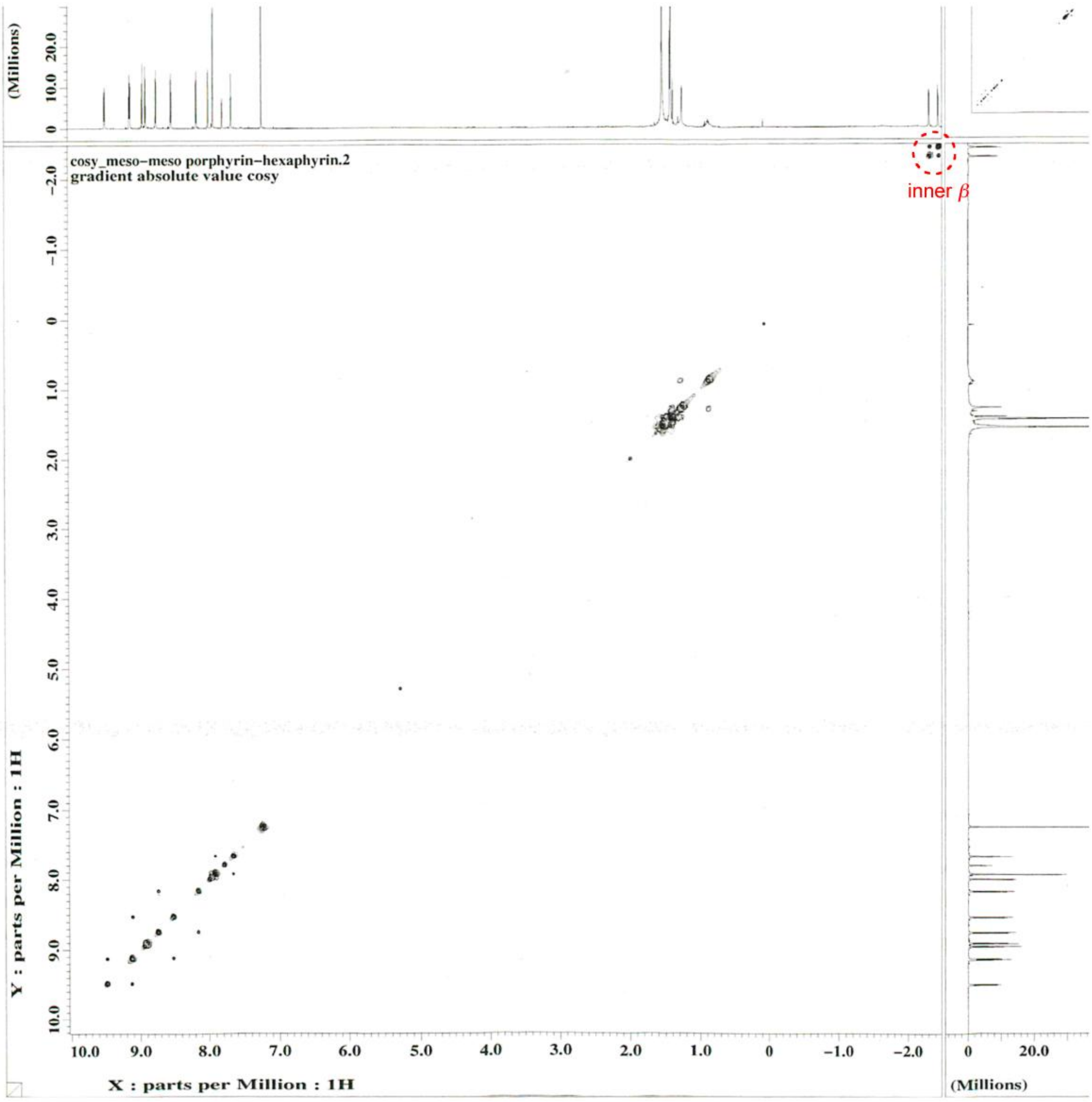

Figure S4. ^{1}H-^{1}H COSY spectrum of **3** in $CDCl_3$ at room temperature.

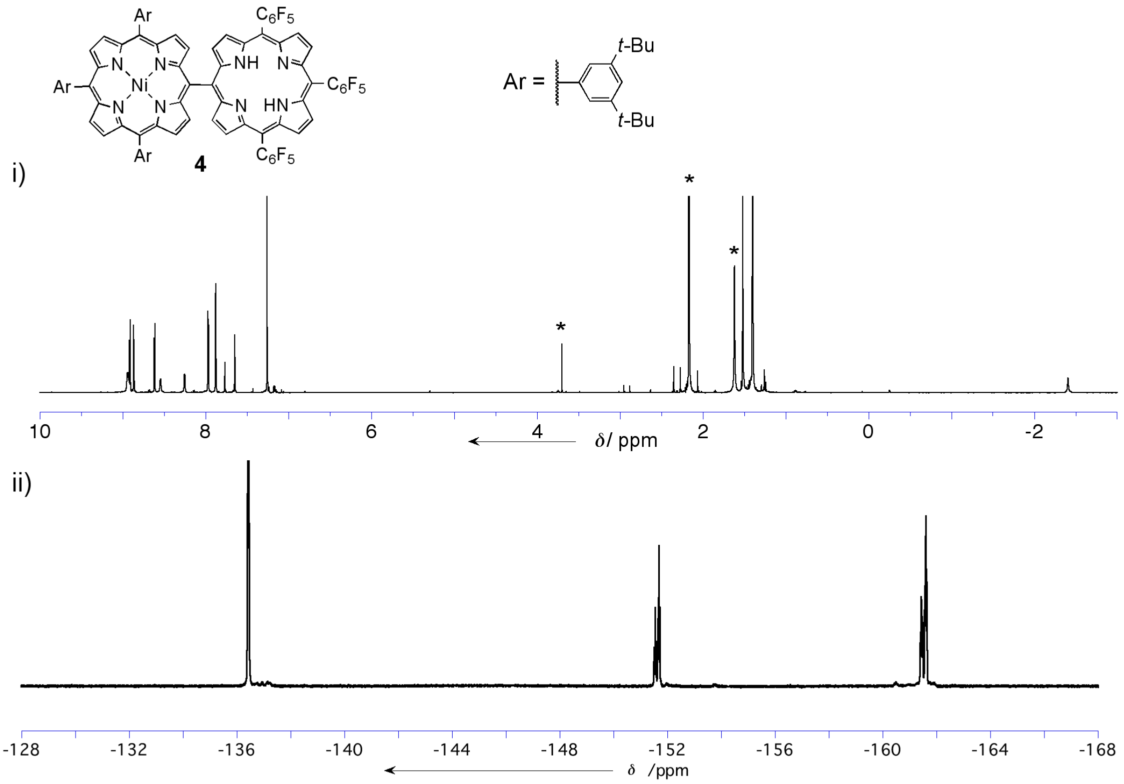

Figure S5. i) ^{1}H and ii) ^{19}F NMR spectra of **4** in $CDCl_3$ at room temperature (*indicate impurity).

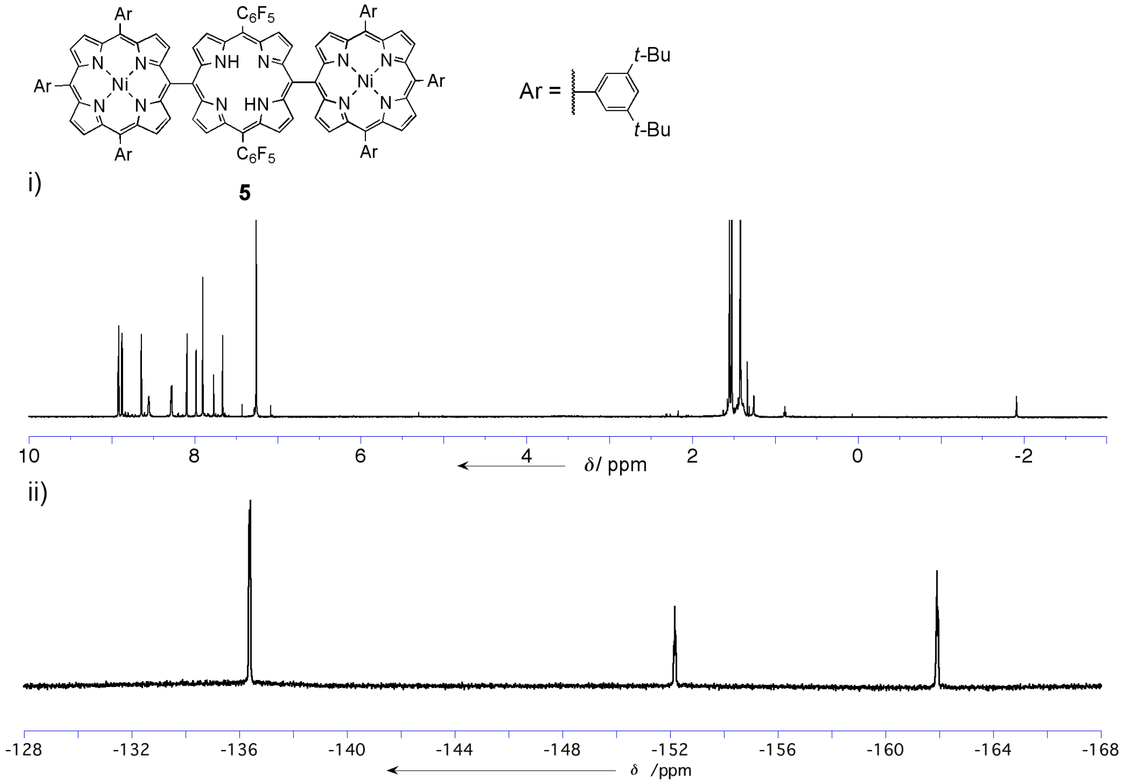

Figure S6. i) ^1H and ii) ^{19}F NMR spectra of **5** in $CDCl_3$ at room temperature.

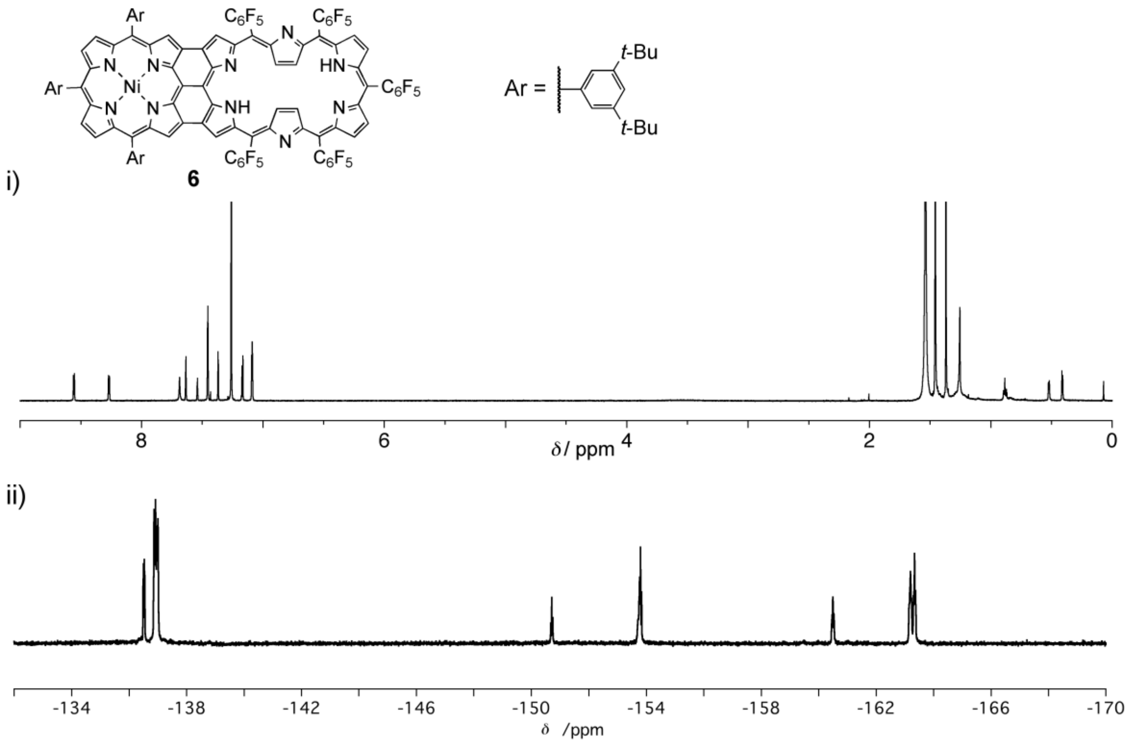

Figure S7. i) ^{1}H and ii) ^{19}F NMR spectra of **6** in $CDCl_3$ at room temperature.

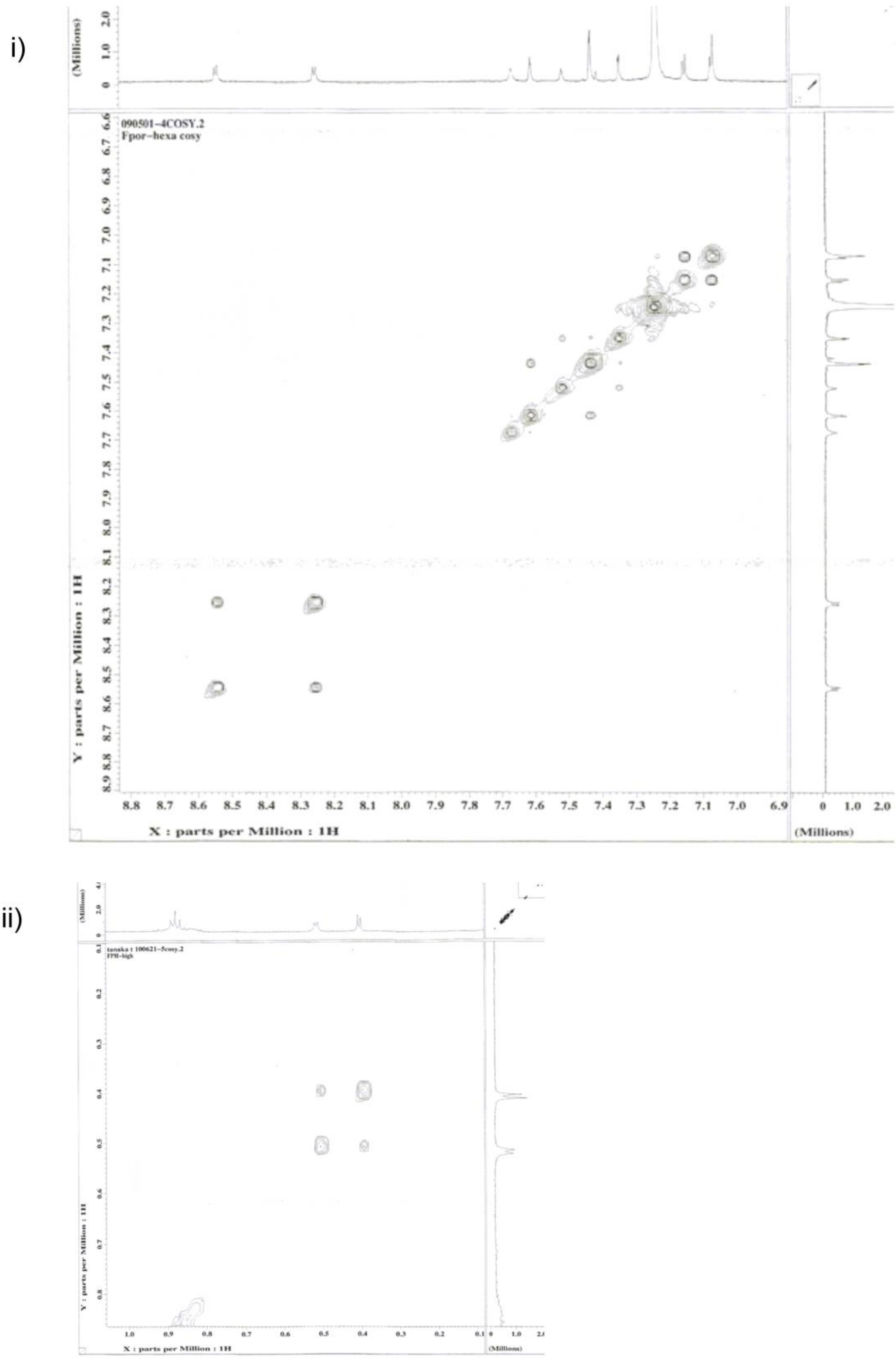

Figure S8. ^{1}H-^{1}H COSY spectra of **6** in $CDCl_3$ at i) 9-7 ppm and ii) 1-0 ppm.

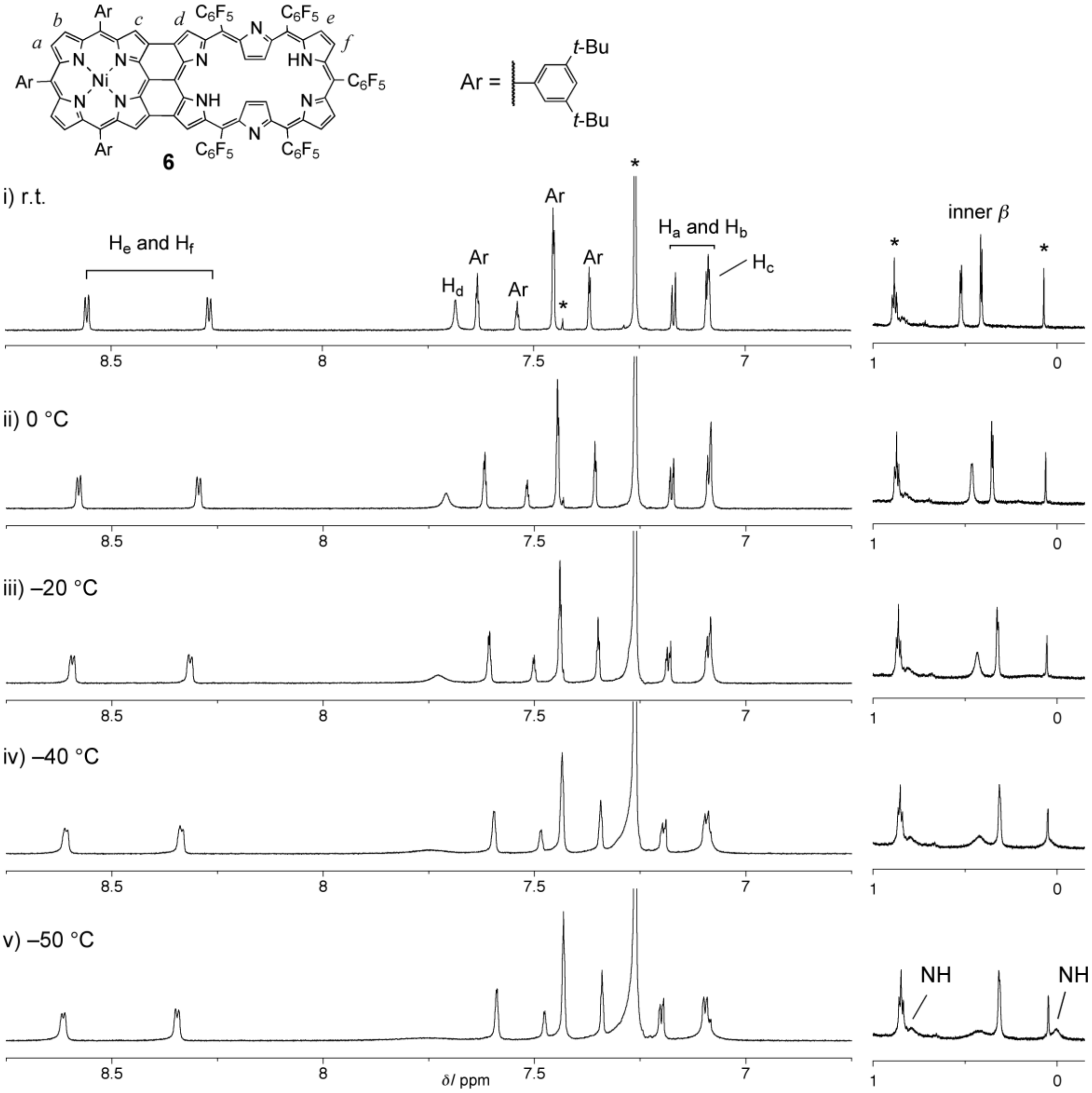

Figure S9. Variable temperature ^{1}H NMR spectra of **6** in $CDCl_3$.

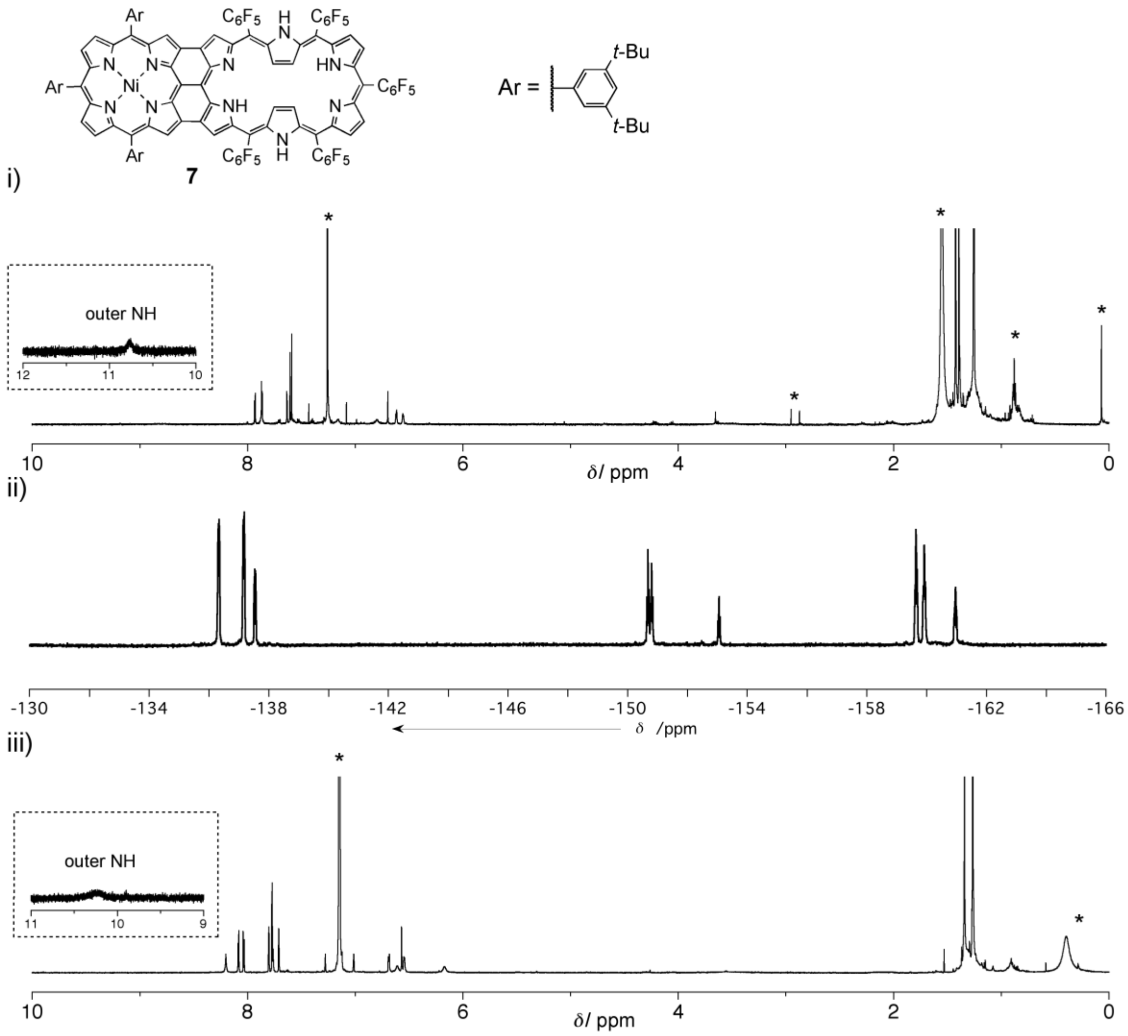

Figure S10. i) ^{1}H and ii) ^{19}F NMR spectra of **7** in $CDCl_3$, and iii) ^{1}H NMR spectrum of **7** in C_6D_6 at room temperature.

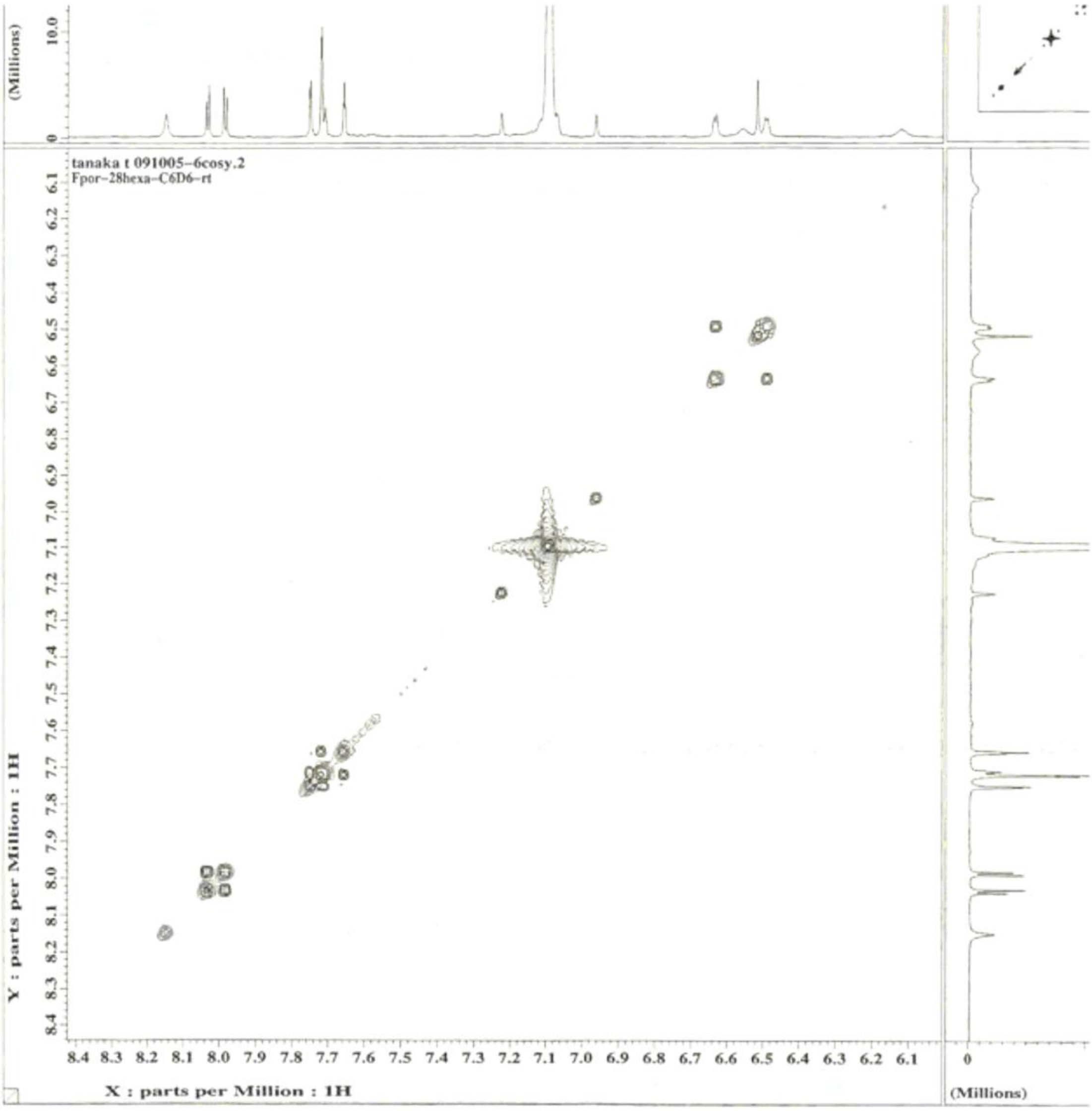

Figure S11. ^{1}H-^{1}H COSY spectrum of **7** in C_6D_6.

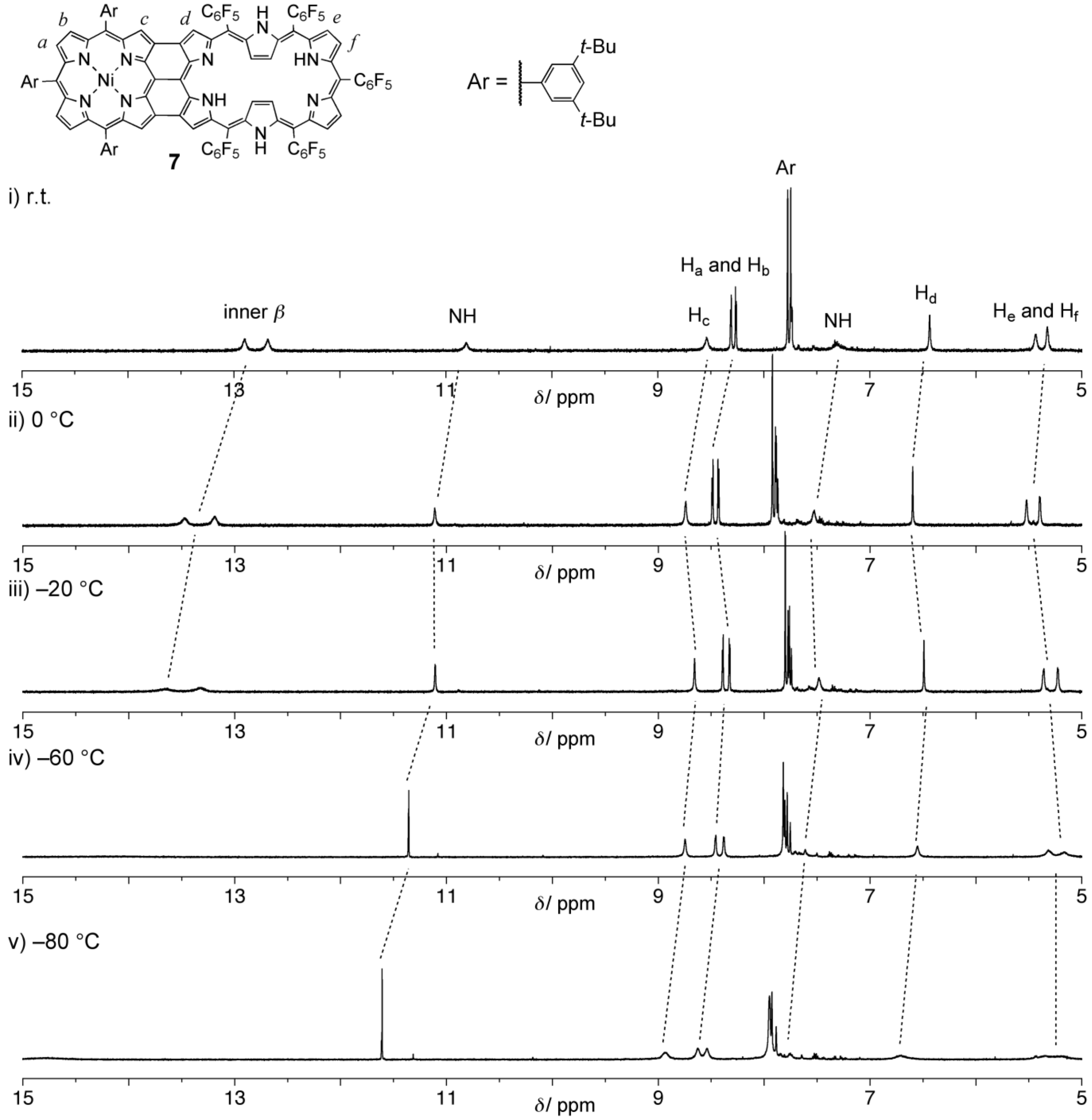

Figure S12. Variable temperature ^{1}H NMR spectra of **7** in [D$_8$]THF.

* When lowering the measurement temperature, the peaks were either broadened or sharpened accompanying with peak shifts to some extent, probably reflecting the subtle balance between increased conformational rigidity at low temperature and desymmetrization due to frozen NH tautomerism. This experiment indicates that any other conformers were not observed in this molecule, thus confirming the main contribution of antiaromatic species.

4. HR-ESI-TOF Mass Spectra

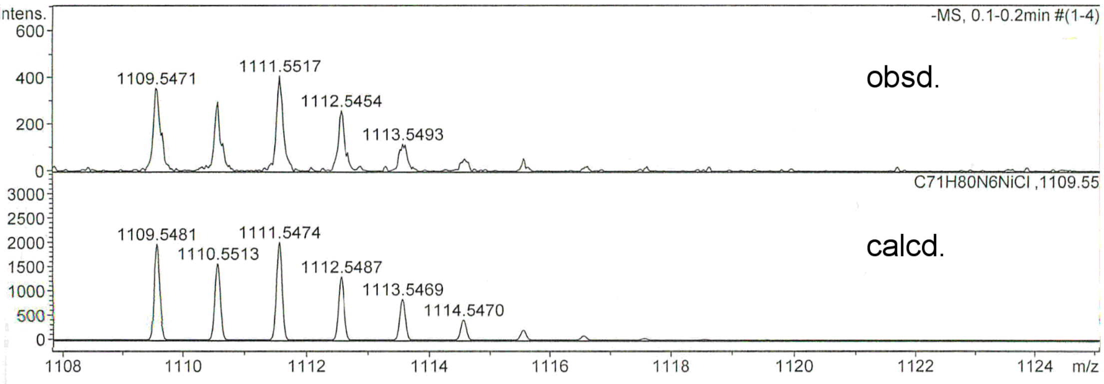

Figure S13. HR-ESI-TOF mass spectrum of **2** (negative-ion mode).

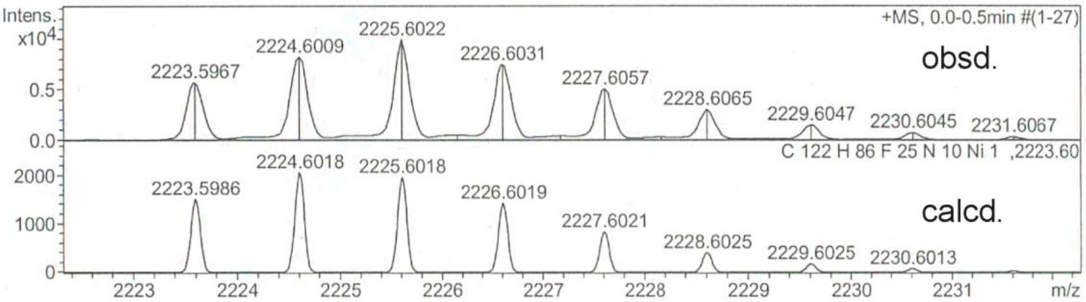

Figure S14. HR-ESI-TOF mass spectrum of **3** (positive-ion mode).

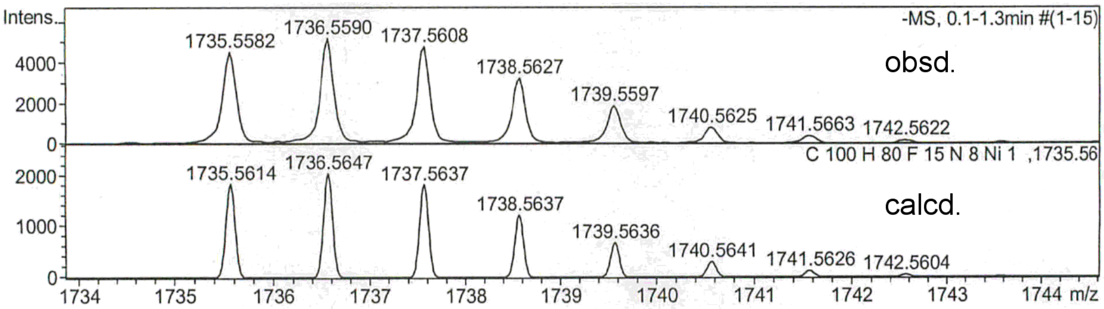

Figure S15. HR-ESI-TOF mass spectrum of **4** (negative-ion mode).

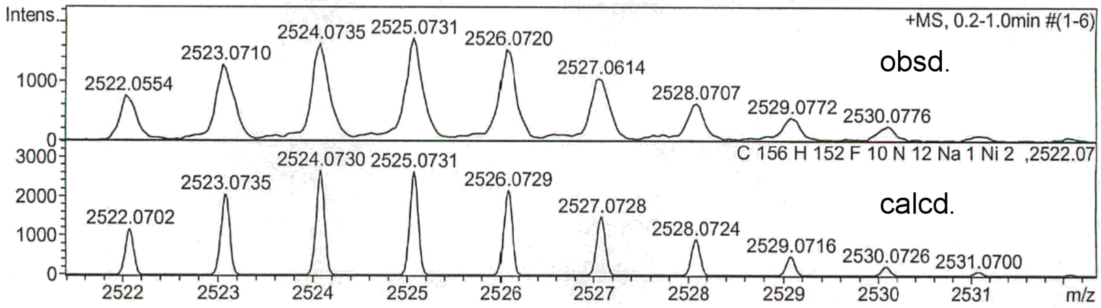

Figure S16. HR-ESI-TOF mass spectrum of **5** (positive-ion mode).

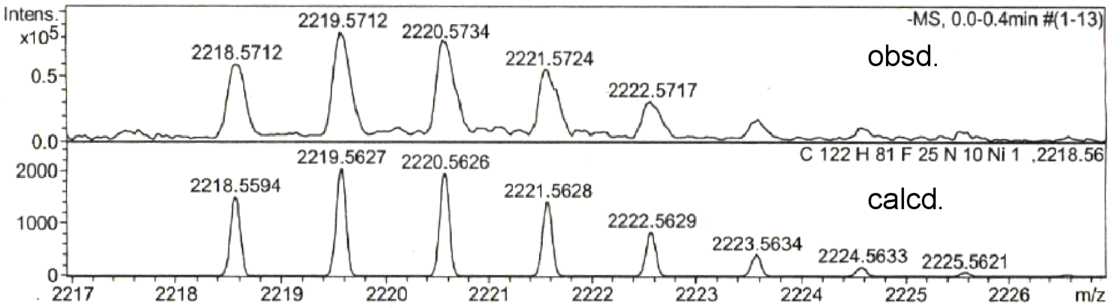

Figure S17. HR-ESI-TOF mass spectrum of **6** (positive-ion mode).

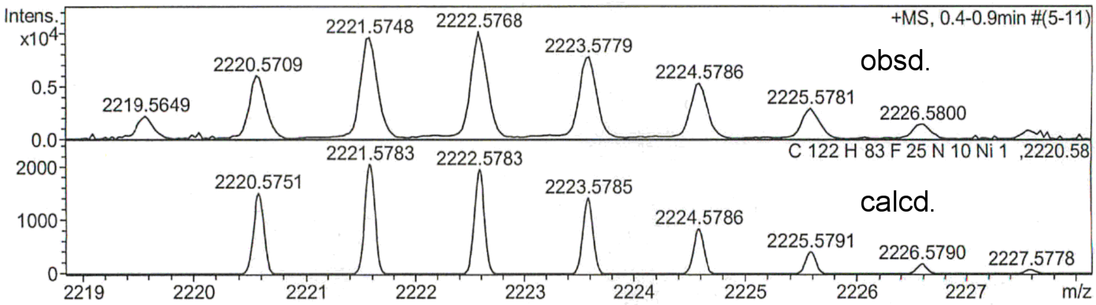

Figure S18. HR-ESI-TOF mass spectrum of **7** (negative-ion mode).

5. Characterizations of Side-product

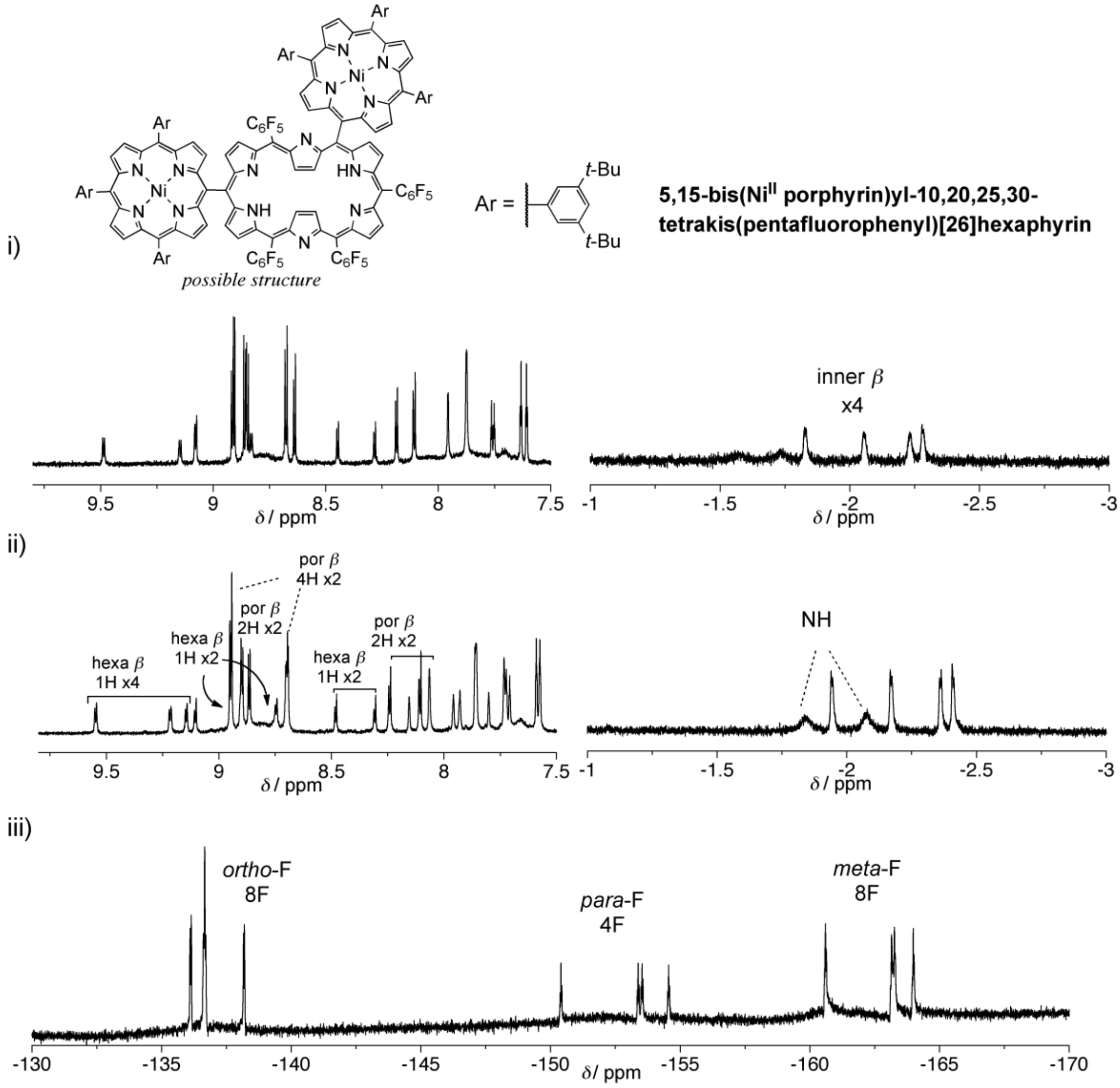

Figure S19. ^{1}H NMR spectra i) at room temperature and ii) at –40 °C, and iii) ^{19}F NMR spectrum at room temperature of **5,15-bis(Ni^{II} porphyrin)yl-10,20,25,30-tetrakispentafluorophenyl [26]hexaphyrin** in $CDCl_3$.

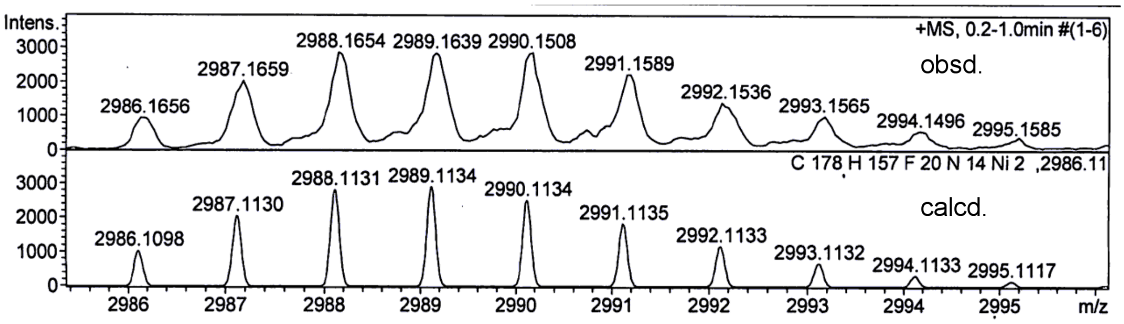

Figure S20. ESI-TOF mass spectrum of **5,15-bis(Ni^{II} porphyrin)yl-10,20,25,30-tetrakispentafluorophenyl [26]hexaphyrin** (positive-ion mode).

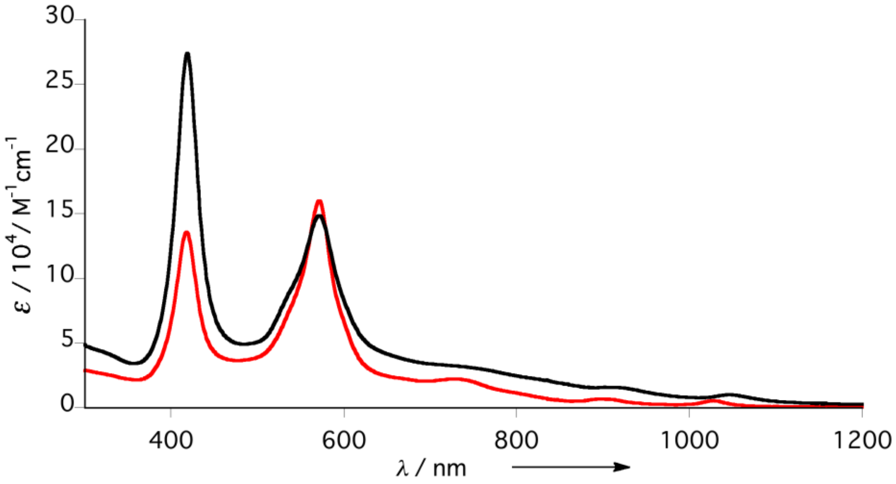

Figure S21. UV/Vis/NIR absorption spectra of **5,15-bis(nickel-porphyrin)yl-10,20,25,30-tetrakispentafluorophenyl [26]hexaphyrin** (black) and **3** (red) in $CHCl_3$.

6. Absorption Spectra

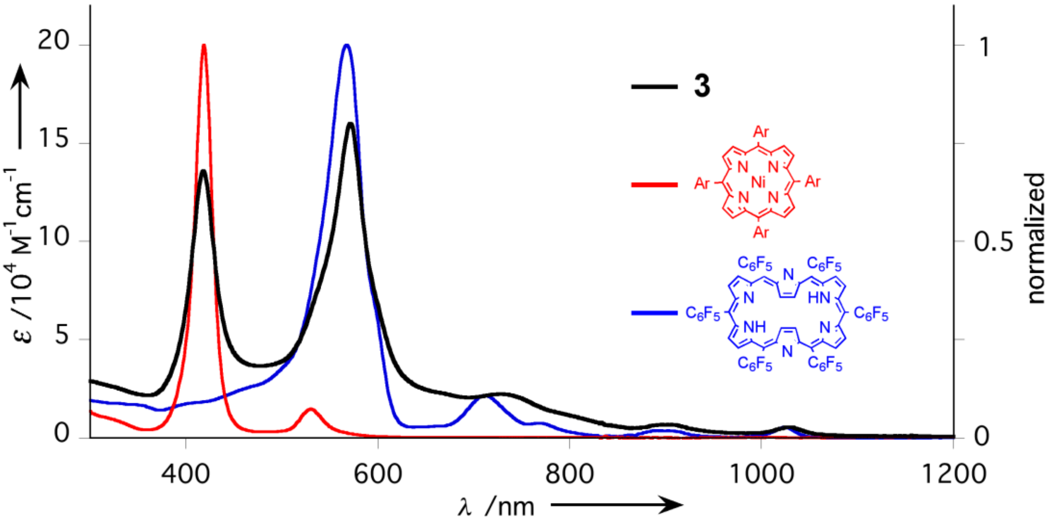

Figure S22. UV/Vis/NIR absorption spectra of **3** (black) and reference molecules (normalized) in $CHCl_3$.

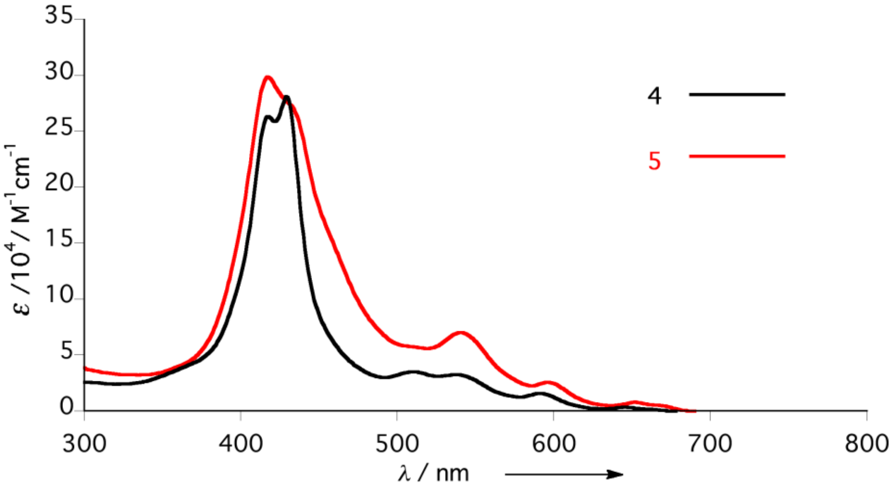

Figure S23. UV/Vis absorption spectra of **4** (black) and **5** (red) in $CHCl_3$.

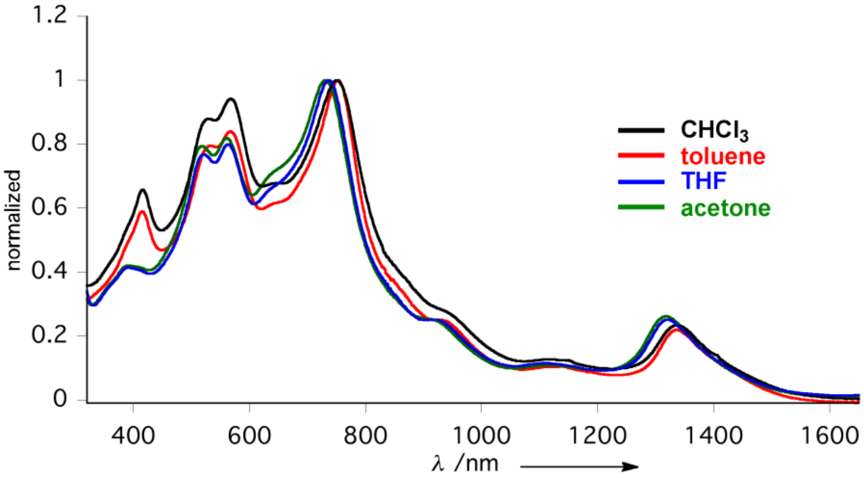

Figure S24. UV/Vis absorption spectra of **6** in various solvents. The absorption intensity was normalized at the peak maxima around 750 nm.

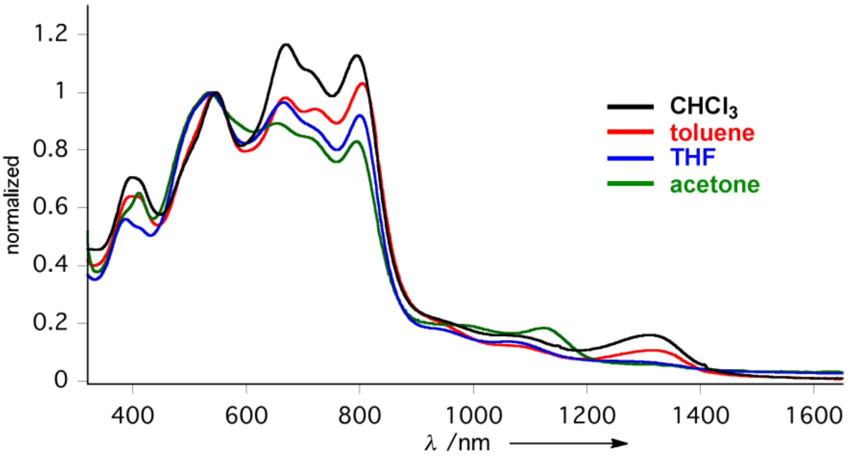

Figure S25. UV/Vis absorption spectra of **7** in various solvents. The absorption intensity was normalized at the peak maxima around 550 nm.

7. Cyclic Voltammetry

*Conditions: electrolytes, Bu_4NPF_6 in CH_2Cl_2, Pt working electrode, Pt wire counter electrode, Ag/$AgClO_4$ reference electrode, scan rate 0.05 V/s. Potentials were also confirmed by using differential pulse voltammetry.

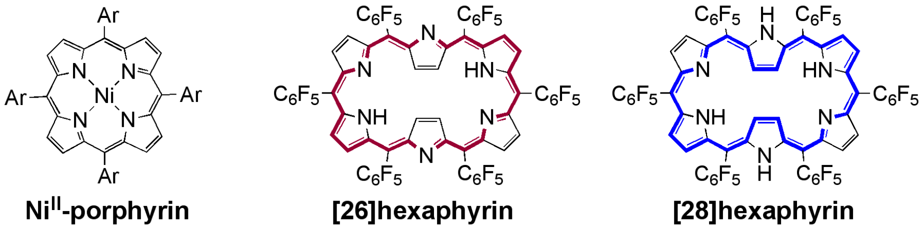

Chrat S1. Reference molecules.

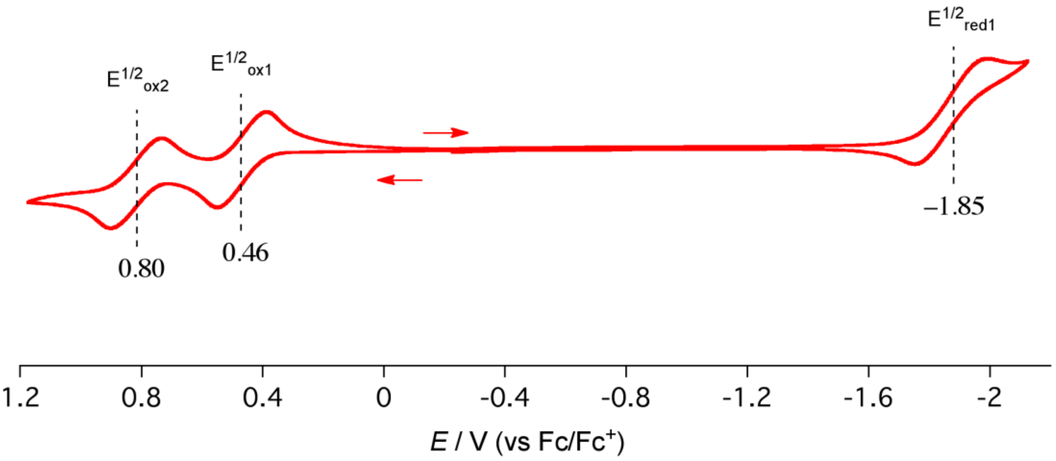

Figure S26. Cyclic voltammogram of **Ni^{II}-porphyrin** measured in CH_2Cl_2. (scan rate = 0.15 V/s)

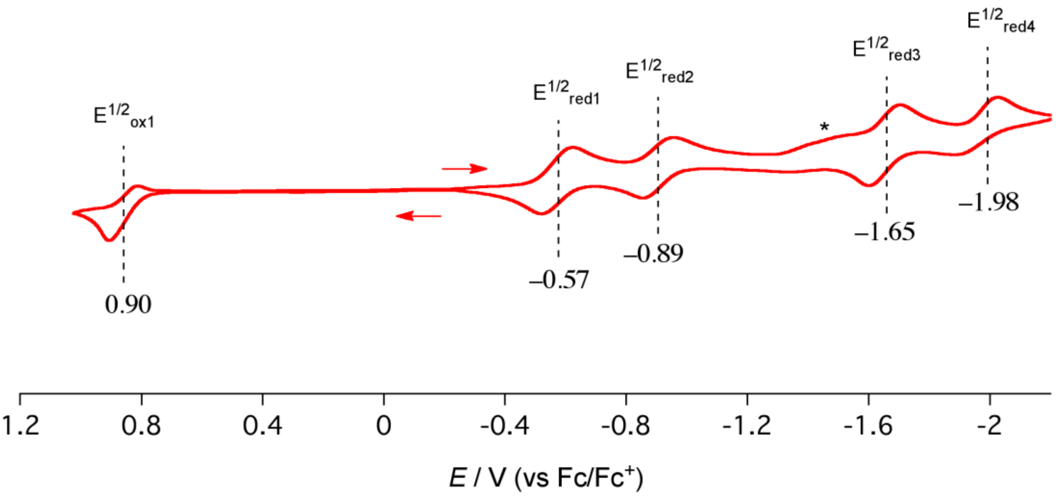

Figure S27. Cyclic voltammogram of **[26]hexaphyrin** measured in CH_2Cl_2.

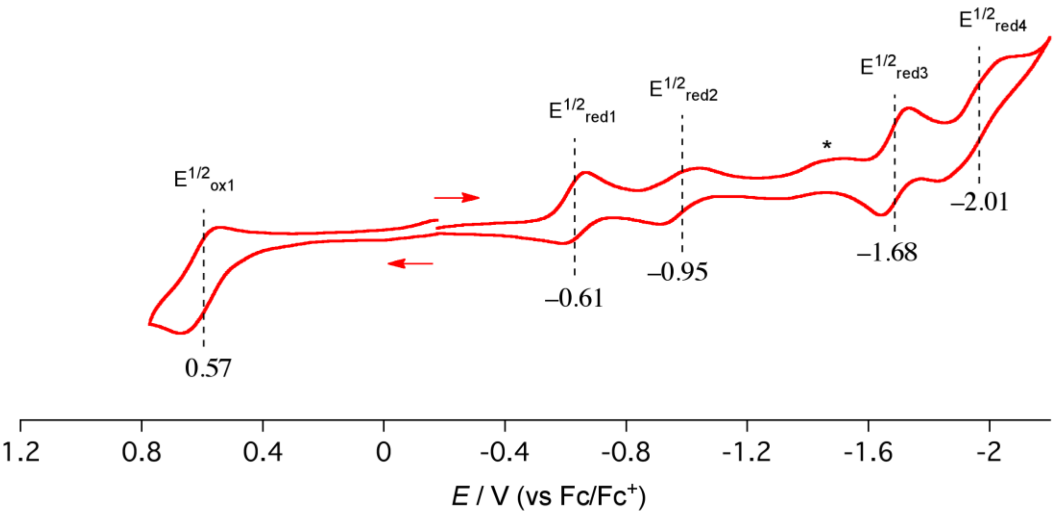

Figure S28. Cyclic voltammogram of **3** measured in CH_2Cl_2.

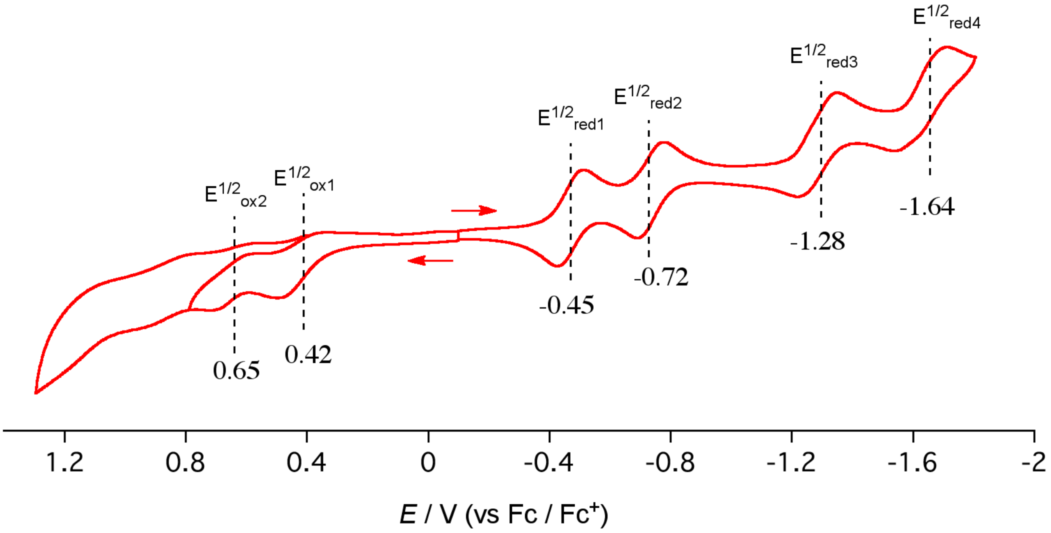

Figure S29. Cyclic voltammogram of **6** measured in CH_2Cl_2.

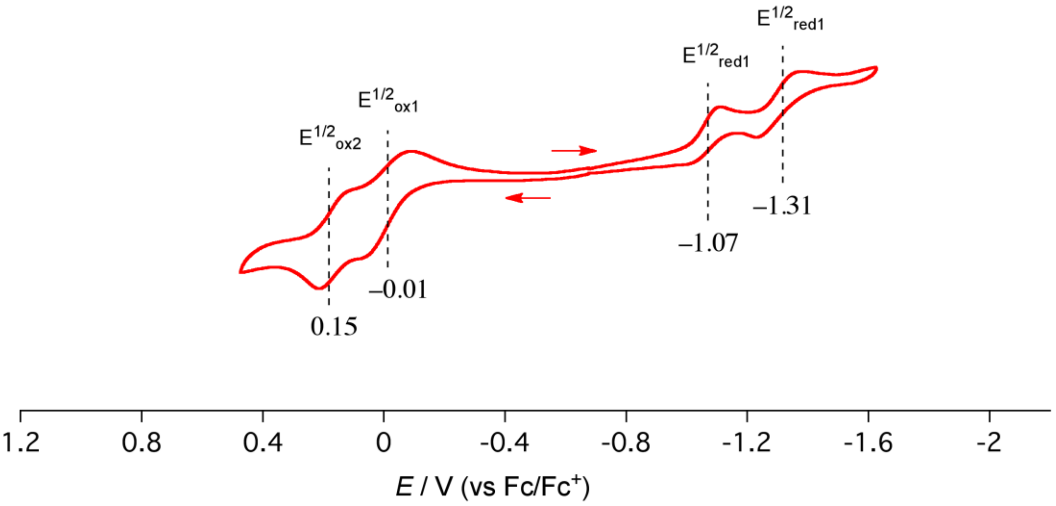

Figure S30. Cyclic voltammogram of **[28]hexaphyrin** measured in CH_2Cl_2.

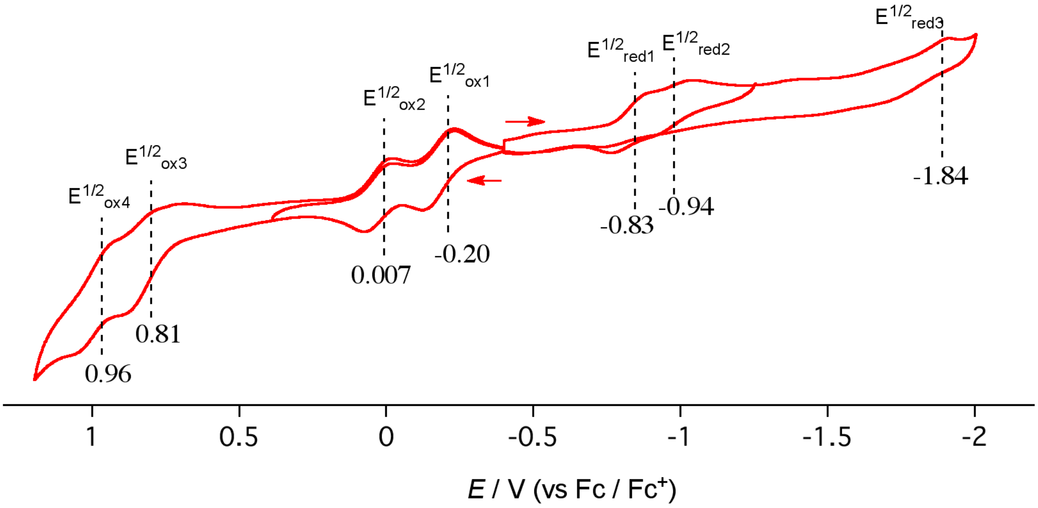

Figure S31. Cyclic voltammogram of **7** measured in CH_2Cl_2.

Table S1. Summary of electrochemical potentials. (a : $E^{1/2}_{ox1} - E^{1/2}_{red1}$)

	$E^{1/2}_{ox4}$ [V]	$E^{1/2}_{ox3}$ [V]	$E^{1/2}_{ox2}$ [V]	$E^{1/2}_{ox1}$ [V]	$E^{1/2}_{red1}$ [V]	$E^{1/2}_{red2}$ [V]	$E^{1/2}_{red3}$ [V]	$E^{1/2}_{red4}$ [V]	HOMO-LUMO gaps [eV] ^{a}
Ni^{II}-porphyrin			0.80	0.46	−1.85				2.31
[26]hexaphyrin				0.90	−0.57	−0.89	−1.65	−1.98	1.47
3				0.57	−0.61	−0.95	−1.68	−2.01	1.18
6			0.65	0.42	−0.45	−0.72	−1.28	−1.64	0.87
[28]hexaphyrin			0.15	−0.01	−1.07	−1.31			1.06
7	0.95	0.81	0.01	−0.20	−0.83	−0.94	−1.84		0.63

8. DFT Calculations.

All calculations were performed at B3LYP/6-31G* (C, H, N, F)/LANL2DZ (Ni) level with Gaussian 09 package.[S1] For optimization, 3,5-di-*tert*-butylphenyl group and pentafluorophenyl group were replaced by 3,5-dimethylphenyl group and 2,6-difluorophenyl group, respectively.

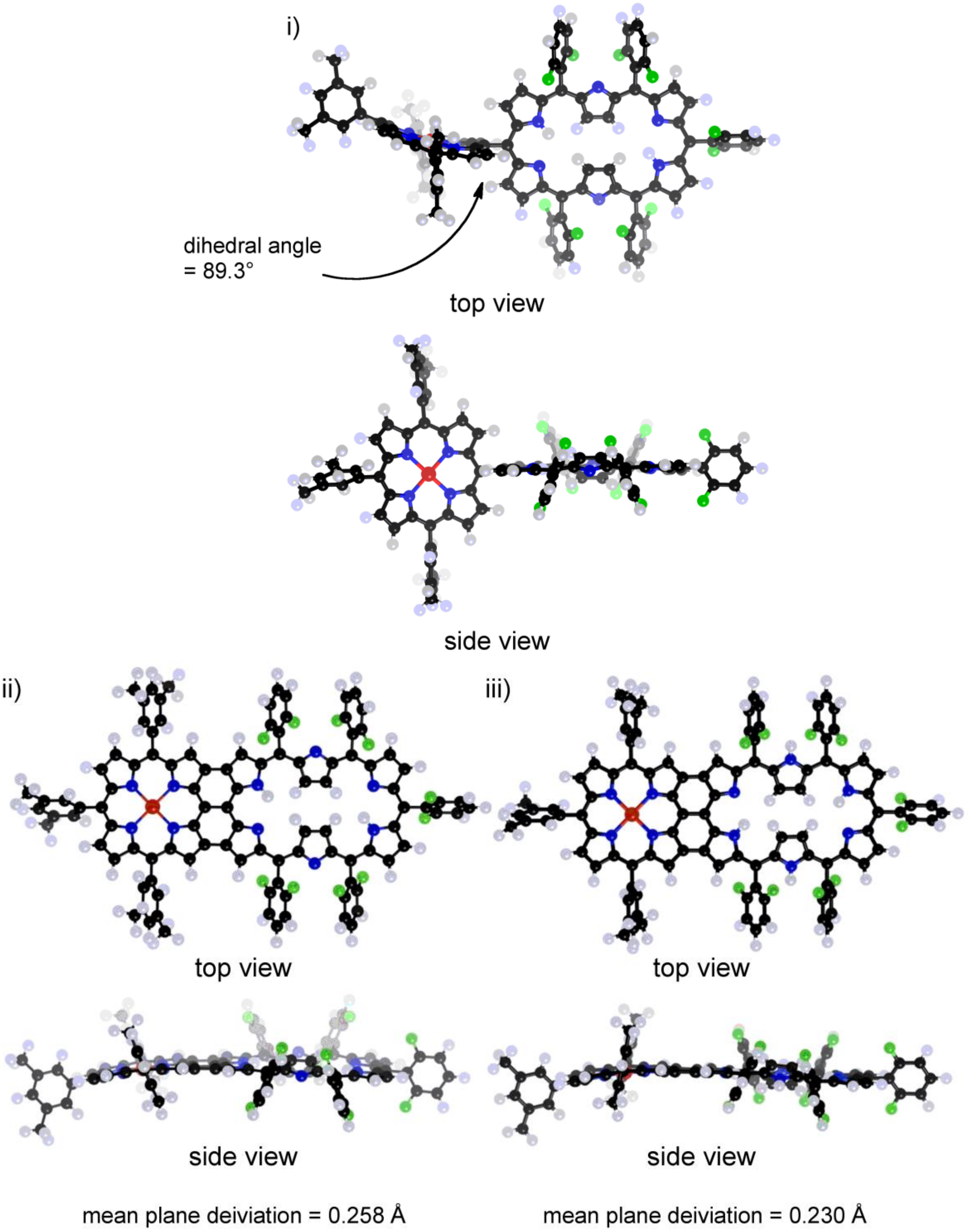

Figure S32. Optimized structures of i) **3**, ii) **6** and iii) **7**.

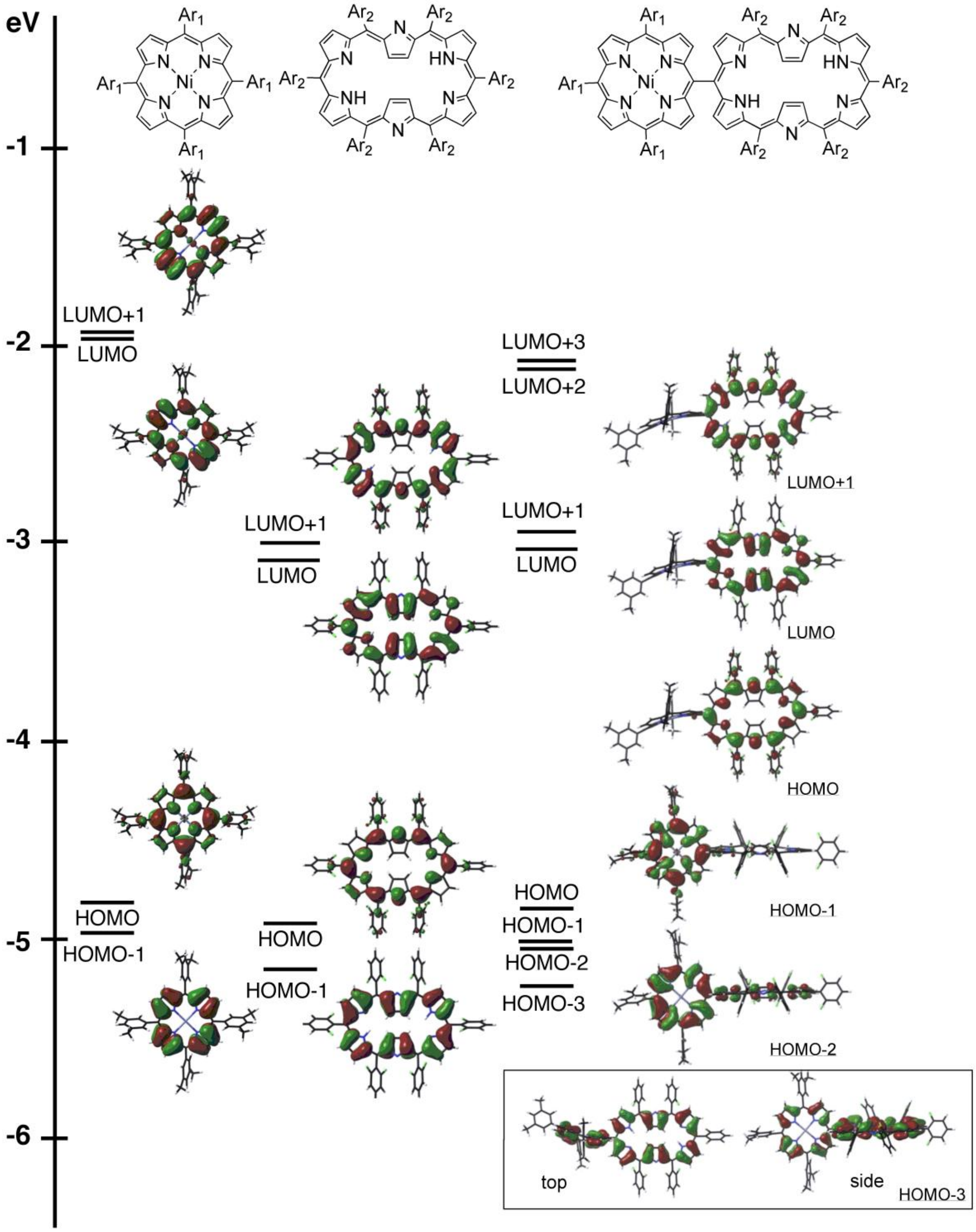

Figure S33. Molecular orbital diagrams of **3** and reference molecules.

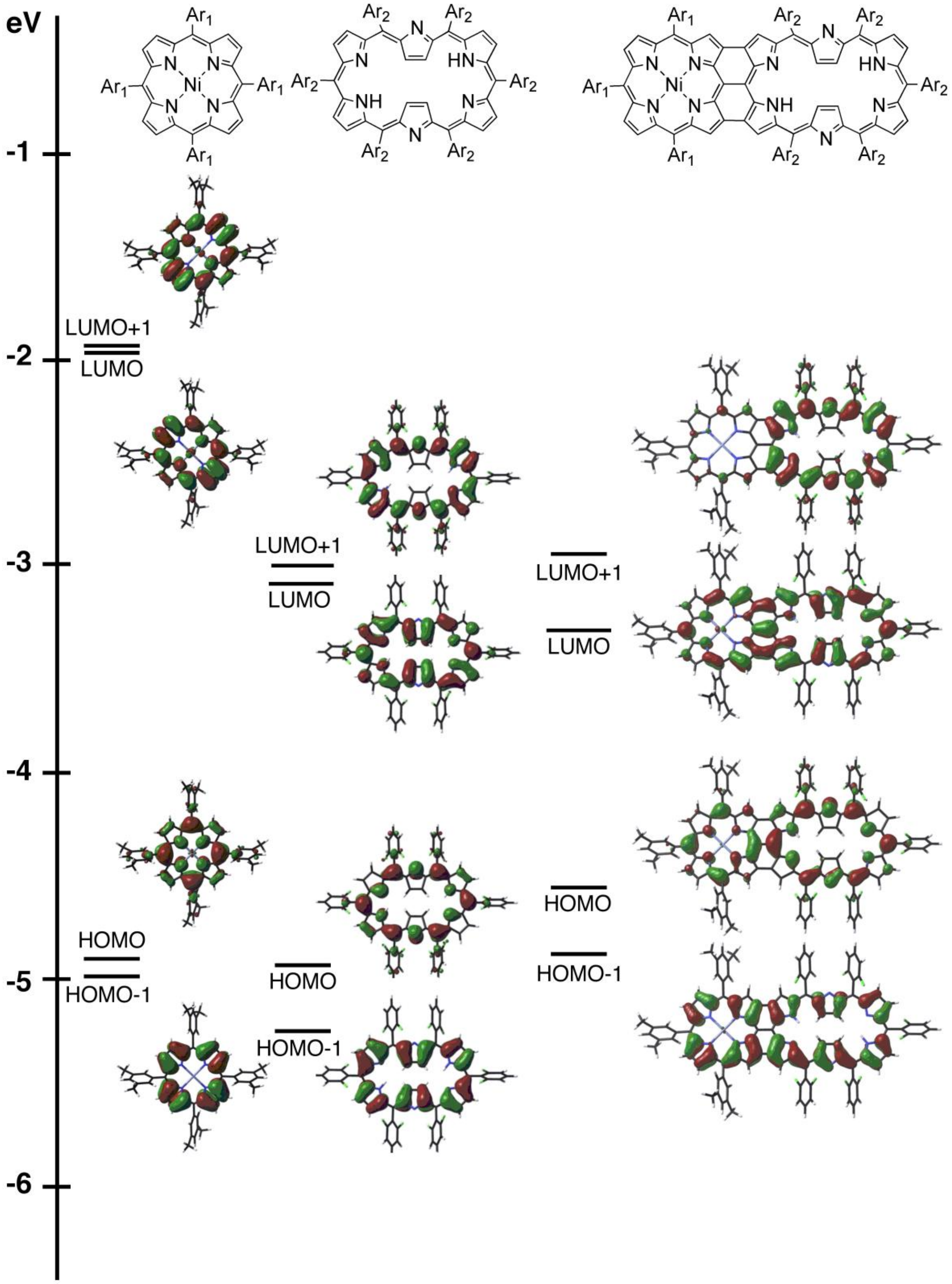

Figure S34. Molecular orbital diagrams of **6** and reference molecules.

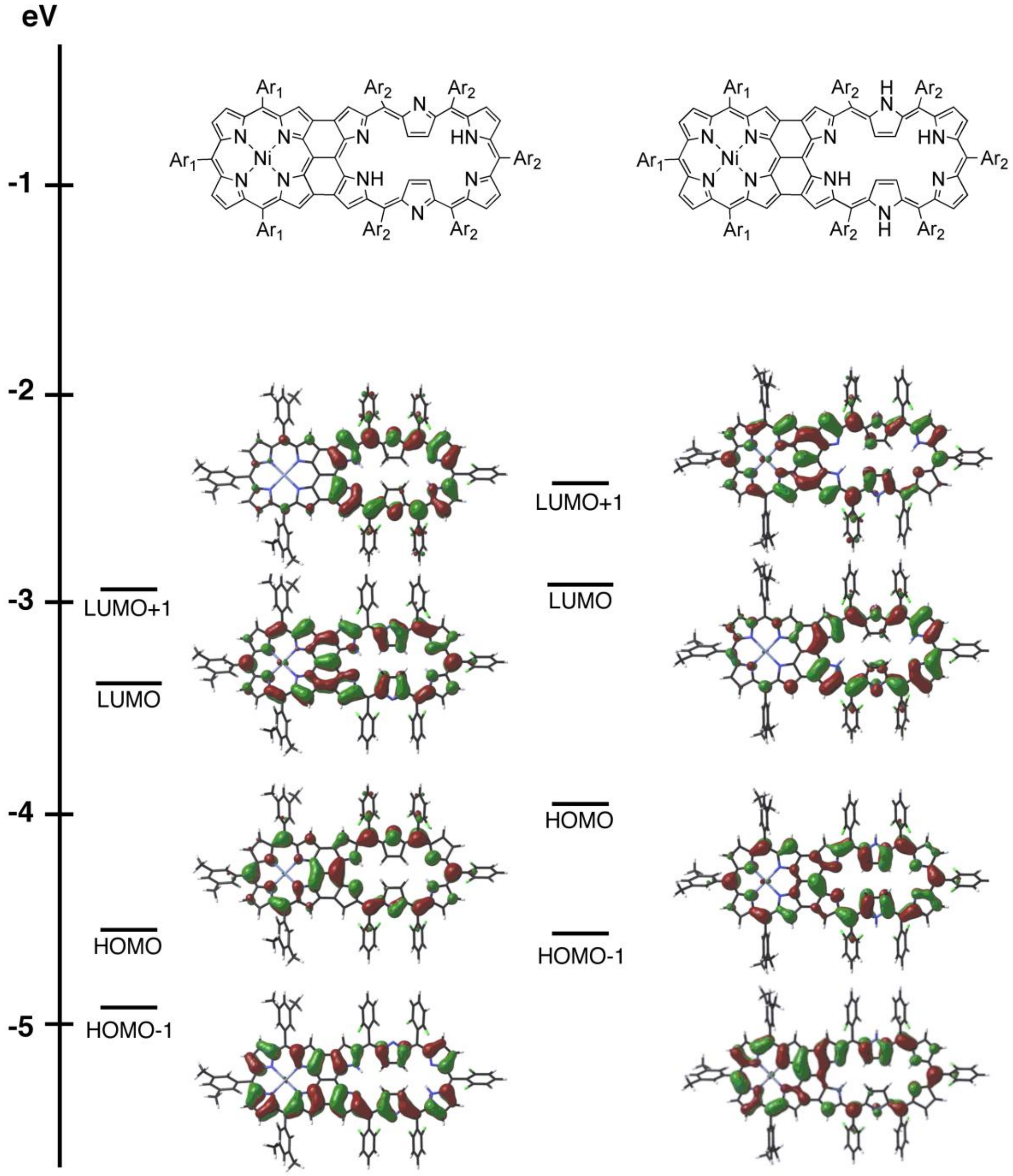

Figure S35. Molecular orbital diagrams of **6** and **7**.

9. Excited State Dynamics

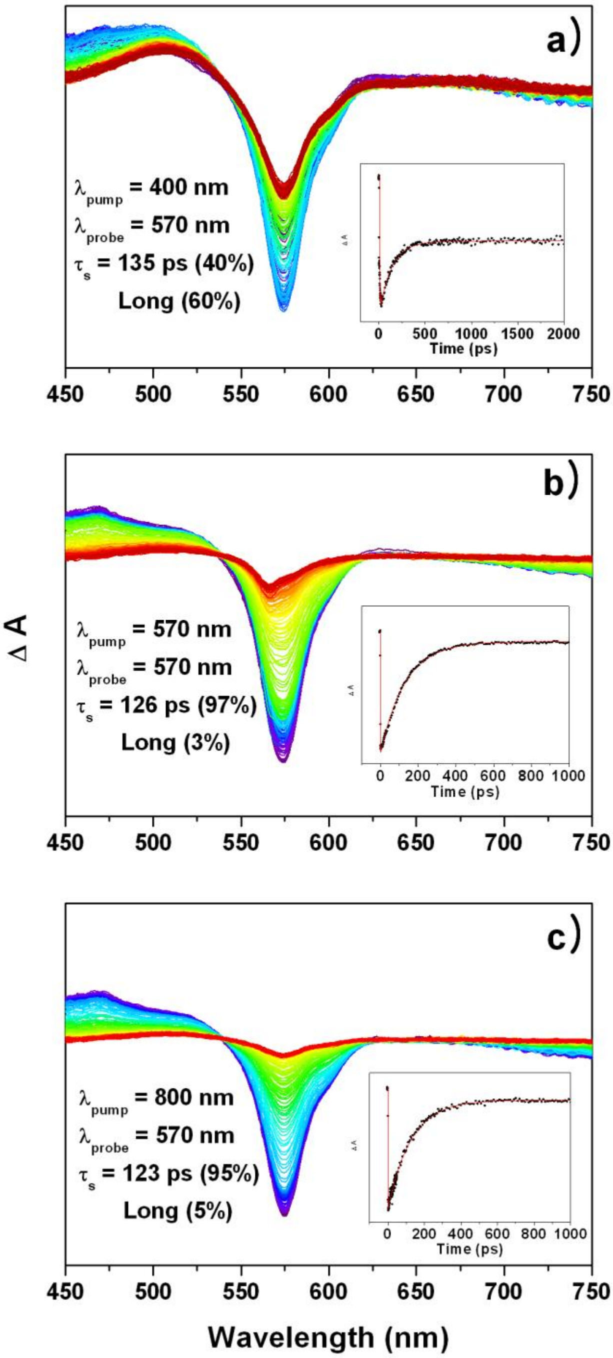

Figure S36. Femtosecond transient absorption spectra and decay profiles of **3** in toluene obtained with 400 (a), 570 (b), and 800 nm (c) excitation.

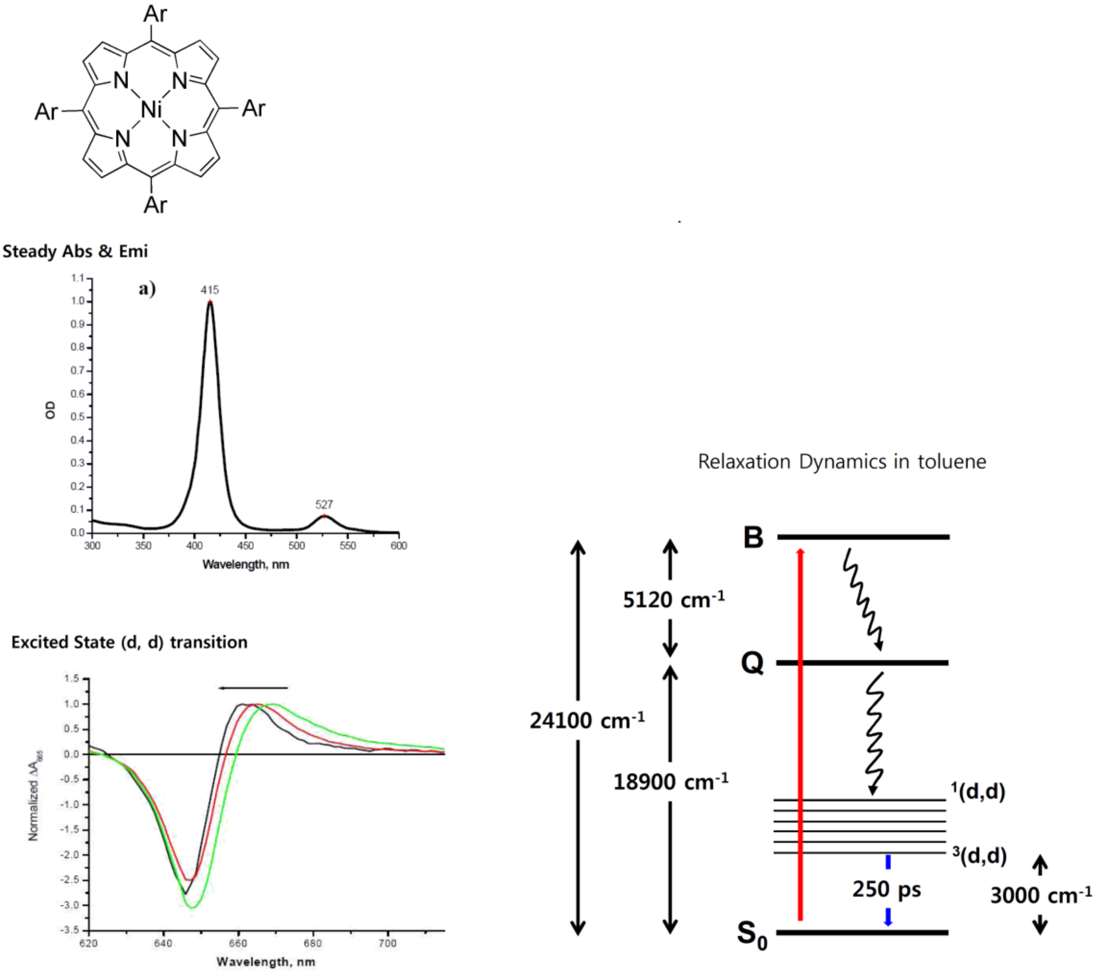
Steady Abs & Emi

Excited State (d, d) transition

Relaxation Dynamics in toluene

Figure S37. Photophysical properties of reference Ni^{II} porphyrin.

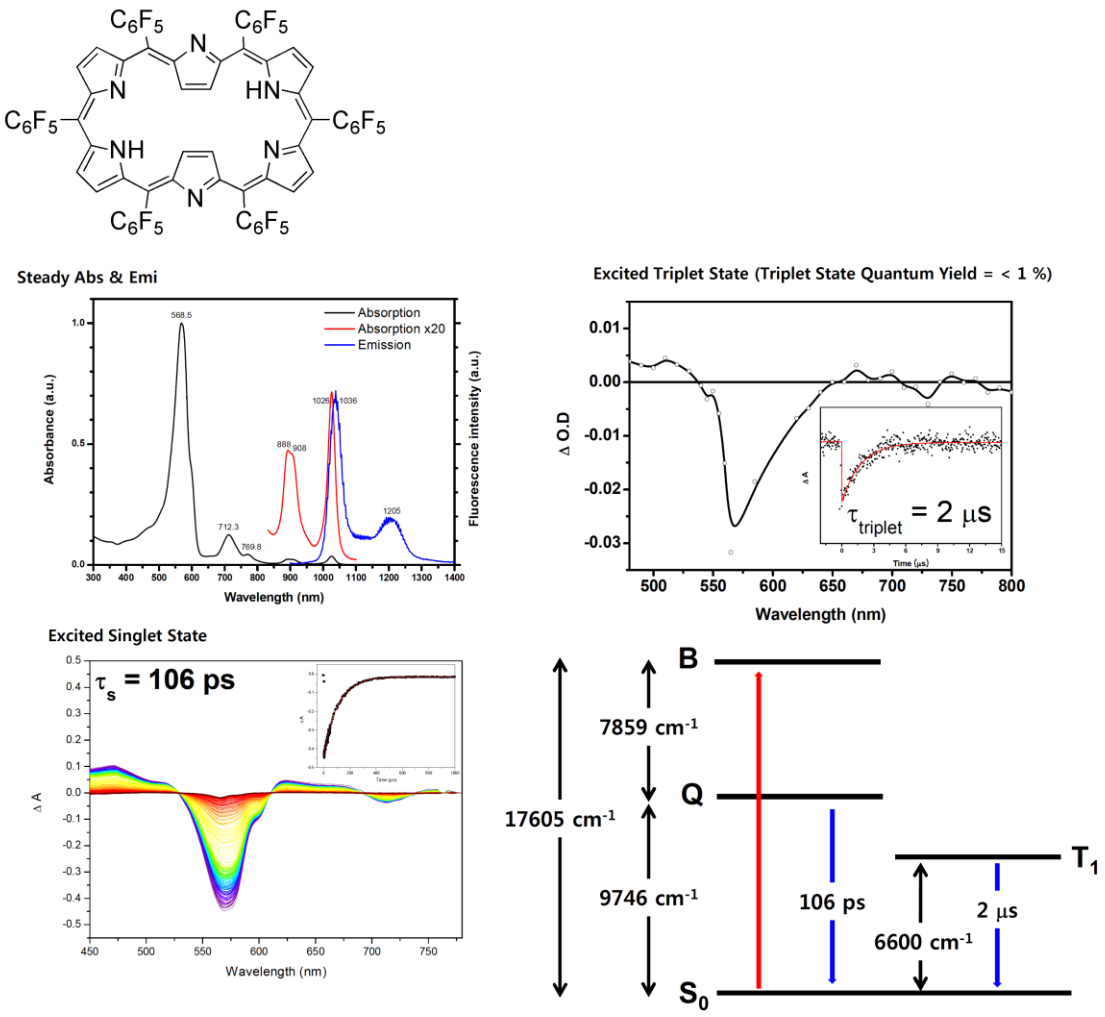

Figure S38. Photophysical properties of reference freebase [26]hexaphyrin.

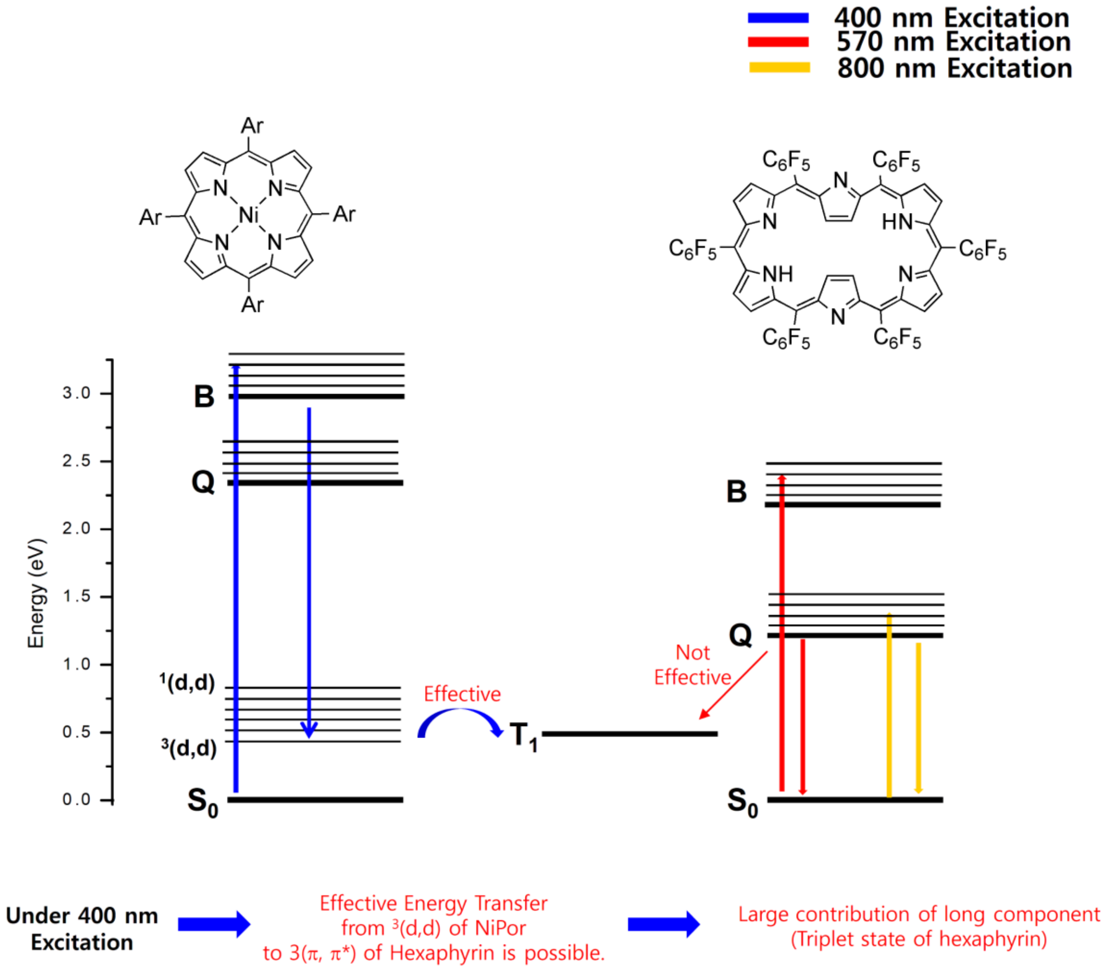

Figure S39. Schematic diagram of the energy relaxation dynamics of **3** under various excitation conditions.

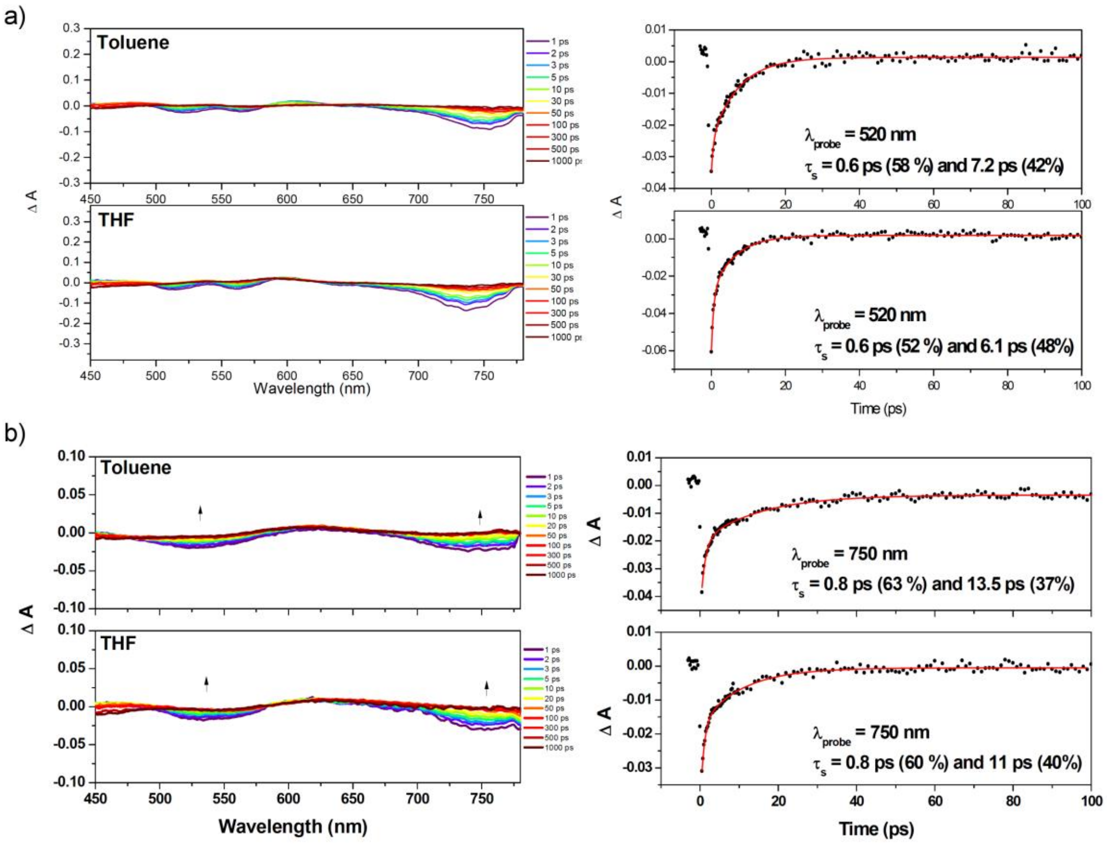

Figure S40. Femtosecond transient absorption spectra and decay profiles of a) **6** and b) **7** in toluene and THF.

10**. Reference.**

[S1] Gausian 09, Revision A. 02,

M. J. Frisch, G. W. Trucks, H. B. Schlegel, G. E. Scuseria, M. A. Robb, J. R. Cheeseman, G. Scalmani, V. Barone, B. Mennucci, G. A. Petersson, H. Nakatsuji, M. Caricato, X. Li, H. P. Hratchian, A. F. Izmaylov, J. Bloino, G. Zheng, J. L. Sonnenberg, M. Hada, M. Ehara, K. Toyota, R. Fukuda, J. Hasegawa, M. Ishida, T. Nakajima, Y. Honda, O. Kitao, H. Nakai, T. Vreven, J. A. Montgomery, Jr., J. E. Peralta, F. Ogliaro, M. Bearpark, J. J. Heyd, E. Brothers, K. N. Kudin, V. N. Staroverov, R. Kobayashi, J. Normand, K. Raghavachari, A. Rendell, J. C. Burant, S. S. Iyengar, J. Tomasi, M. Cossi, N. Rega, J. M. Millam, M. Klene, J. E. Knox, J. B. Cross, V. Bakken, C. Adamo, J. Jaramillo, R. Gomperts, R. E. Stratmann, O. Yazyev, A. J. Austin, R. Cammi, C. Pomelli, J. W. Ochterski, R. L. Martin, K. Morokuma, V. G. Zakrzewski, G. A. Voth, P. Salvador, J. J. Dannenberg, S. Dapprich, A. D. Daniels, O. Farkas, J. B. Foresman, J. V. Ortiz, J. Cioslowski, and D. J. Fox, Gaussian, Inc., Wallingford CT, 2009.